ASTRON. OBS.

OCT 11 1927

TWELFTH ANNUAL MEETING OF THE OPTICAL SOCIETY OF AMERICA
SCHENECTADY, N. Y., OCTOBER 20, 21, AND 22, 1927.

Volume 15 Number 4

Journal
of the
Optical Society of America
and
Review of Scientific Instruments

EDITOR-IN-CHIEF: PAUL D. FOOTE
THE MELLON INSTITUTE OF INDUSTRIAL RESEARCH, UNIVERSITY OF PITTSBURGH, PITTSBURGH, PA.
ASSISTANT EDITOR-IN-CHIEF AND BUSINESS MANAGER: F. K. RICHTMYER
CORNELL UNIVERSITY, ITHACA, N. Y.
CONSULTING BUSINESS MANAGER: M. E. LEEDS, PHILADELPHIA, PA.

Associate Editors:

Term Ending Dec. 31, 1931	Term Ending Dec. 31, 1929	Term Ending Dec. 31, 1927
FRANK ALLEN	E. C. CRITTENDEN	H. D. CURTIS
K. T. COMPTON	HERBERT E. IVES	WILLIAM DUANE
K. K. DARROW	R. A. MILLIKAN	PAUL E. KLOPSTEG
G. S. FULCHER	L. P. SIEG	L. SILBERSTEIN
I. C. GARDNER	J. P. C. SOUTHALL	L. T. TROLAND
L. A. JONES	H. S. UHLER	F. E. WRIGHT

OCTOBER, 1927

The Scattering of Light in Amorphous Solids – – – – – – C. V. RAMAN 185
The Photomagnetic Effect in Silver Chloride and in Selenium – – C. W. HEAPS 190
Photo-elastic Properties of Transparent Cubic Crystals – – – H. B. MARIS 194

INSTRUMENT SECTION

Photo-elastic Investigations of the Tensil Test Specimen, the Notched Bar, the Ship Propeller Strut, and the Roller Path Ring – – – – – H. B. MARIS 203
A Potentiometer Arrangement for the Measurement of Emf over a Wide Range – – – – – – – – – – – – – – – – C. D. MILLER 238
Reviews – – – – – – – – – – – – – – – – – – – 189, 201
Notes – 246
Index to Advertisers – – – – – – – – – – – – – – – Cover III

Published Monthly by the
OPTICAL SOCIETY OF AMERICA

OFFICE OF PUBLICATION
GEORGE BANTA PUBLISHING COMPANY
450-454 Ahnaip St.,
MENASHA, WISCONSIN

Entered as second-class matter May 31, 1921, at the postoffice at Menasha, Wis., under the Act of March 3, 1879. Acceptance for mailing at special rate of postage provided for in the Act of February 28, 1925, embodied in paragraph 4, section 412, P. L. and R. authorized June 19, 1925.

Journal
of the
Optical Society of America
and
Review of Scientific Instruments

Published monthly by the Optical Society of America in cooperation with the Association of Scientific Apparatus Makers of the United States of America. The Section on Optics is devoted to original papers on experimental, theoretical, and applied optics. The Section on Scientific Instruments is devoted to original papers on instruments of all kinds (electrical, mechanical, thermal, etc., as well as optical) for research, instruction, and industrial processes. Manuscripts for publication are invited, whether authors are members of the Optical Society or not.

Annual subscription $5.00 dating from January of current year. Single copies $0.60. Back numbers: Vols. 1–5 (The Journal of the Optical Society, 1917–1921 inclusive) $16.00. Vol. 6–7, $5.00 per volume; Vol. 8—, $2.50 per volume. Address publishers, "George Banta Publishing Company, 450–454 Ahnaip Street, Menasha, Wisconsin, or F. K. Richtmyer, Manager, Cornell University, Ithaca, New York," for all correspondence regarding subscriptions, back numbers, changes of address, advertising rates and accounts, and missing numbers.

THE OPTICAL SOCIETY OF AMERICA

President—W. E. FORSYTHE, Nela Research Laboratories, Cleveland, Ohio.
Vice-President—I. G. PRIEST, Bureau of Standards, Washington, D. C.
Secretary—C. C. BIDWELL, Cornell University, Ithaca, N. Y.
Treasurer—ADOLPH LOMB, Rochester, New York.

The Council consists of the above officers, the Editor-in-Chief and the Assistant Editor-in-Chief and Business Manager of the JOURNAL, the past President, Herbert E. Ives, Bell Telephone Laboratories, Inc., and the following elected members: K. T. Compton, Princeton University; Carl W. Keuffel, Keuffel and Esser Co., C. E. K. Mees, Eastman Kodak Co.; P. G. Nutting, Geological Survey.

The object of the Optical Society of America is to serve the interests of all who are engaged in any branch of optics from fundamental research to the manufacture of optical goods.

The Constitution provides that any one who has contributed materially to the advancement of optics shall be eligible to regular membership in the Society with the privilege of voting and holding office. Any individual or corporation interested in optics is eligible to associate membership. Annual dues including subscription to the JOURNAL are five dollars for individual associate membership, seven dollars and fifty cents for individual regular membership and fifty dollars for corporation membership. Further information may be obtained from the Secretary.

Rochester, N. Y., Section of the Optical Society of America.

President—F. M. BISHOP, *Secretary*—L. V. FOSTER,
Vice-President—S. STERLING, *Treasurer*—E. E. RICHARDSON,
Councilors: F. C. FAIRBANKS, H. F. KURTZ, A. J. NEWTON, W. B. RAYTON

Journal
of the
Optical Society of America
and
Review of Scientific Instruments

Vol. 15 OCTOBER, 1927 Number 4

THE SCATTERING OF LIGHT IN AMORPHOUS SOLIDS

By C. V. Raman

1. INTRODUCTION

Recent investigations have shown that when light traverses a dust-free liquid, an observable fraction of the energy is laterally scattered and that this effect is due to the local fluctuations of density and to the random orientations of the molecules which cause the fluid to be optically inhomogeneous.[1] In the case of a mixture of liquids, we have in addition a scattering due to the local fluctuations of composition which cause corresponding local variations of refractive index. Since the transverse scatterings due to density and composition fluctuations are fully polarized, while that due to the random orientation of the molecules is almost entirely unpolarized, the resultant scattering in a fluid is usually only partially polarized. When the temperature of a liquid is lowered, its compressibility usually diminishes and with it also the local fluctuations of density. Thus we may expect that when the liquid is cooled to such an extent that it passes into the amorphous solid condition, the density scattering would become very small. On the other hand, in liquid mixtures, the local fluctuations of *composition* usually tend to increase rather than to diminish with fall of temperature. Thus they should certainly tend to persist or even increase when the mixture congeals into an amorphous solid. The effect due to random molecular orientations would certainly remain in the amorphous solid condition. Thus, we may anticipate that an amorphous solid such as glass consisting of a mixture of anisotropic molecules would exhibit when light traverses it, a partially-polarized internal scattering or opalescence of an order of intensity not greatly inferior to that ordinarily observed in liquids or liquid mixtures.

[1] C. V. Raman, Molecular Diffraction of Light, Calcutta University Press, 1922.

An internal scattering of light in common glasses and also in optical glasses has actually been noticed.[2] Its nature has been a subject of debate,[3] and owing to our insufficient knowledge of the amorphous state, is not fully understood at present. Judging, however, from such observations as are available, it is the opinion of the writer, that the effect observed in optical glasses is a true molecular scattering arising from local fluctuations of composition and of molecular orientation, being thus of the same general nature as the opalescence observed in binary liquid mixtures such as phenol-water, carbon disulphide-methyl alcohol and so on. In support of this view, it is proposed in this paper to give the results of the study of the light-scattering in a series of 14 different optical glasses manufactured by the firm of Schott in Jena.[4] If the light-scattering in glass were due to accidental inclusions or incipient crystallizations occurring within it as has been suggested by some writers, we should expect the intensity of the scattered light to show large and arbitrary variations depending on the circumstances of the particular melting from which the specimen was taken. On the other hand, if the phenomenon has a true molecular origin, we should expect to find the intensity of scattering to be definitely correlated with the refractivity and chemical constitution of the glass.

TABLE 1. *List of classes examined.*

	Melting	Type	Composition	Refractive index μ	$\nu = 1/\omega$
No. 1	18165	0.6781	Fluor crown	1.4933	69.9
2	4927	U. V. 3199	U. V. crown	1.5035	64.4
3	15189	0.144	Borosilicate crown	1.5100	64
4	16564	0.3832	Prism crown	1.5163	64
5	15065	0.3453	Silicate crown	1.5191	60.4
6	16740	0.3439	Telescopic flint	1.5286	51.6
7	16397	0.7550	Baryta light flint	1.5694	56
8	14657	0.211	Densest Borosilicate crown	1.5726	57.5
9	17538	0.340	Ordinary Light flint	1.5774	41.4
10	18023	0.1266	Baryta light flint	1.6042	43.8
11	11095	0.103	Ordinary flint	1.6202	36.2
12	10259	0.748	Baryta flint	1.6235	39.1
13	8988	0.102	Dense flint	1.6489	33.8
14	16889	0.198	Densest flint	1.7782	26.5

[2] Lord Rayleigh, Proc. Roy. Soc., *95*, p. 476, 1919, and C. V. Raman, "Molecular Diffraction of Light," p. 85.

[3] R. Gans, Ann. der Phys., *77*, p. 317; 1925.

[4] The specimens were presented by Messrs. Schott to Prof. P. N. Ghosh, who kindly placed them at the writer's disposal for the work.

2. THE SPECIMENS EXAMINED

Table 1 gives a list of the glasses examined and their description as furnished by the manufacturers, arranged in order of increasing refractive index. The samples were furnished in the form of slabs 7 cm×7 cm×2 cm, with one pair of end-faces polished. For the purpose of the observation of light-scattering, the slabs were immersed in a trough containing benzene and a beam of sunlight focused by a lens was admitted through a side-face, the necessity of polishing the latter being thus avoided. The track of the beam as seen through the end-faces was perfectly uniform and appeared of a beautiful sky-blue color.

3. EXPERIMENTAL RESULTS

When the scattered light was viewed through a double-image prism held so that the direction of vibrations in the two images seen were respectively perpendicular and parallel to the direction of the beam traversing the glass, it was seen that these were of very different intensities, showing that the scattered light was strongly but not completely polarized. The color of the stronger image was always a sky-blue. The color of the fainter image in the ordinary flint glasses was blue, but in the other specimens varied very considerably. The total intensity of the scattered light in the glasses was determined by comparison with that of the track in a bulb containing dust-free benzene immersed in the same trough as the block of glass under examination and traversed by the same beam of light. A rotating-sector photometer was used for the purpose. The ratio of the intensities in the parallel and perpendicular components of vibration in the laterally scattered light was also determined with the help of a double-image prism and nicol (Cornu's method) in the usual way. The measurements give us the ratio of the intensity of the faint image to the bright image seen through the double image prism, and this expresses the degree of depolarization of the scattered light.

The results of the work are gathered together in Table 2.

4. DISCUSSION OF RESULTS

From a scrutiny of the figures in Table 2, several interesting facts emerge. In the first place, it will be seen that the crown glasses show uniformly a smaller intensity of light-scattering than the other varieties of glass. Both the ordinary flints and the baryta flints scatter light strongly, the latter more so than ordinary flints of equal refractive index. It will be seen also that considering each species of glass sepa-

rately, there is a progressive increase of the intensity of light-scattering with increasing refractive-index. The colors shown by the fainter components of the scattered light in the first four glasses in Table 2 are obviously due to a species of weak fluorescence, probably of the same kind as has been met with in investigations on light-scattering in liquids.[5] This fluorescence being unpolarized, the large values of the depolarization found in the case of these glasses stands self-explained. If the fluorescent light had been excluded by the introduction of

TABLE 2. *Experimental results.*

	Glass	Refractive index	Color of bright component	Color of faint component	Depolarization	Intensity relative to benzene = 1
No. 1	Fluor crown	1.4933	Blue	Yellow	0.180	0.18
2	U. V. crown	1.5035	"	Pink	0.158	0.12
3	Borosilicate crown	1.5100	"	"	0.295	0.11
4	Prism crown	1.5163	"	"	0.285	0.14
5	Silicate crown	1.5191	"	Blue	0.123	0.18
6	Telescopic flint	1.5286	"	Purple	0.068	0.40
7	Baryta light flint	1.5694	"	"	0.053	0.44
8	Densest borosilicate crown	1.5726	"	"	0.045	0.37
9	Ordinary light flint	1.5774	"	Indigo-blue	0.067	0.30
10	Baryta light flint	1.6042	"	Indigo	0.067	0.41
11	Ordinary flint	1.6202	"	Blue	0.079	0.42
12	Baryta flint	1.6235	"	Indigo-blue	0.085	0.57
13	Dense flint	1.6489	"	Blue	0.062	0.52
14	Densest flint	1.7782	"	"	0.065	0.63

suitable color-filters, the depolarization for these glasses would have been much smaller. It is interesting to notice that in glasses Nos. 6, 7, and 8, we have a low value for the depolarization in spite of the obvious presence of a weak fluorescence; this is obviously due to the greater intensity of polarized scattering appearing in the last column of Table 2 of these glasses.

The several regularities to which attention has been drawn above, particularly the fact that the intensity of scattering is very clearly a function of the refractive-index and chemical composition of the glass, render it extremely improbable that the effect can arise from accidental inclusions or imperfections in the structure of the glasses. It is, in fact, clear from the data that the effect arises from the ultimate molecular structure of glass.

[5] K. S. Krishnan, Phil. Mag., *50*, p. 697; 1925.

It would be very interesting to study the light-scattering in amorphous solids having a relatively simple chemical constitution, e.g., transparent quartz-glass. Experiments on the scattering of light in liquids which can first be rendered dust-free and then supercooled into the amorphous solid state may also be expected to furnish important information. Further work on these lines is in progress.

210 BOWBAZAR STREET,
CALCUTTA, INDIA,
MAY 11, 1927.

Statics and the Dynamics of a Particle. By William D. MacMillan, Professor of Astronomy at the University of Chicago. xviii+430 pages. The McGraw-Hill Book Company. New York. $5.00.

According to the preface, this is the first of a series of volumes in this general field, the present volume being "designed as a text-book in mechanics for . . . . students in our colleges and universities, particularly those students who are interested in astronomy, physics, or mathematics" and for "that relatively small group of engineers who wish to extend their knowledge beyond the mere rule of thumb into the deeper foundations of general theory."

The book is divided into three parts: I, The Fundamental Concepts of Mechanics; II, Statics; III, The Dynamics of a Particle. Each part is divided into chapters, sixteen in all, which have such chapter headings as Vectors; Velocity; Acceleration; Mass and Force; Work and Energy; The Statics of a Particle; Moments of Vectors; Virtual Work; Elastic Solids; Gravity and Acceleration; Curvilinear Motion; Constrained Motion; The Generalized Coordinates of Lagrange; Hamilton's Equations; etc.

While the book is best suited to the student of Mathematics, Physics or Astronomy who is well past elementary courses, the presentation is most admirable—in that it starts from the elementary and proceeds rapidly, but with adequate though concise discussion, to the more advanced. Thus, it is a long journey from the problem (page 33) "A stone dropped over a cliff strikes the ground in 5 sec. With what speed did it strike . . . . ?" to the problem (page 344) "Find the time required for a body to slide down the curve

$$\frac{x^2}{a^2} = \frac{4}{9}\left(\frac{z}{a} - 1\right)^3$$

assuming . . . . ."

The author, however, very skillfully directs the student along the road.

Incidentally, the book contains very many excellent problems—a feature which, in conjunction with the well written text, should recommend the book for general use.

F. K. RICHTMYER

THE PHOTOMAGNETIC EFFECT IN SILVER CHLORIDE AND IN SELENIUM

By C. W. Heaps

It has been observed by Garrison[1] that the magnetic susceptibility of silver halides is altered by exposing these substances to light from a tungsten lamp. The phenomenon, which he designates as a "photomagnetic effect," is supposed to be due to the transition of the molecule to a condition of increased electric moment under the action of light. This increase of polarity is associated with a change of magnetic properties.

The writer has performed some experiments on silver chloride and on selenium, and has failed to detect the existence of any photomagnetic effect in either substance. Nevertheless, the negative result of the experiments is not unimportant,—some interesting conclusions may be drawn regarding the nature of the diamagnetic susceptibility coefficient.

EXPERIMENT

A light-sensitive, diamagnetic bar of selenium was prepared by the usual casting and annealing process. This bar was fixed across the end of a light glass rod carrying a mirror, and the system was suspended by a quartz fibre from a torsion head and enclosed in a brass chamber from which the air could be pumped. A window in the chamber allowed light to fall upon the bar. Through this window another beam of light was reflected from the mirror on to a scale 115 cm away.

The brass chamber was supported between the conical pole-pieces (4.1 cm apart) of a Weiss electromagnet and the torsion head adjusted so that the bar made an angle of approximately 45° with the line joining the tips of the conical pole-pieces. The period of the suspended system was 110 seconds when the magnetic field was zero. The torsion head had to be turned through 803° to keep the needle position constant when a field of 200 gauss was produced at the center of the needle. The field was, of course, very non-uniform. Under these conditions a twist of the torsion head of 0.5° produced a deflection of 1 mm on the scale. Light from a 100 watt tungsten lamp was then transmitted through a 25 cm water cell and focussed by a large lens upon the selenium. No deflection as large as one mm was produced. We may thus

[1] Allen Garrison, Journal Amer. Chem. Soc., *47*, pp. 622–626; 1925.

conclude that the torsion head twist required to balance any photomagnetic effect was less than 0.5°. If ϕ is the torsion head twist to balance the torque of the field and $\delta\phi$ the change of ϕ to balance the photomagnetic effect we may write, in view of the above observations, $\delta\phi/\phi < 0.00062$.

In the case of silver chloride a bar was made by Garrison's method, the salt being produced by precipitation from a solution of silver nitrate. The bar was diamagnetic, and the torsion head twist required to balance the torque of the field was 787°. In this case a field of 640 gauss was used. In the field a twist of 0.74° of the torsion head produced one mm deflection of the spot of light. Illuminating the bar with the 100 watt lamp arranged as described above produced no deflection so large as 2 mm. This was about the smallest amount which could nave been observed with certainty. Thus, for silver chloride, $\delta\phi/\phi < 0.00188$.

It should be mentioned that certain disturbing factors had to be eliminated in these experiments. Preliminary observations gave an apparent photomagnetic effect which was quite large. Subsequent tests, however, showed that radiometer action and radiation pressure effects were responsible for these deflections. A hot soldering iron caused quite a large deflection, which began without an appreciable time lag after the iron was held before the window of the apparatus. By altering the direction of the heat rays incident on the suspended system this deflection could be made zero or reversed in direction.

When light from the lamp was filtered through the water cell and the angle of incidence properly adjusted there was no effect to be observed in zero magnetic field. Under these conditions when the bar was in the field any motion produced by the incident light could be attributed to a change of magnetic susceptibility.

The air pressure in the chamber was 7 cm of mercury for the selenium and less than one mm for the silver chloride.

For an apparatus of the kind described above it may be shown that the torque produced on the bar by the field is proportional to the difference of susceptibilities of the bar and the surrounding gas. In our case the gas pressure was so small that its susceptibility may be neglected compared with that of the bar. Thus the torque of the field is proportional to the susceptibility, k, of the bar. A change, δk, produced in k by light, necessitates a change, $\delta\phi$, in ϕ to prevent any motion. Obviously $\delta\phi/\phi = \delta k/k$. It thus appears that $\delta k/k < 0.00062$ for selenium, and $\delta k/k < 0.00188$ for silver chloride.

After the above described experiments were performed the effect of light on the electrical conductivity of selenium was determined. The bar was removed from the chamber and placed, in series with a battery and galvanometer, so as to receive the same illumination as was previously used when it was in the chamber. This illumination was found to produce an increase of conductivity of about 35%.

DISCUSSION

Most theories of the action of light on selenium agree basically in attributing its affect to the freeing of electrons; that is, electrons which in the dark are confined to the force field of a particular molecule, in the light are free to go from one force field to another. We may in this sense say that the number of free electrons in selenium is increased by illumination.

Now according to one viewpoint free electrons in a metal contribute to its diamagnetic susceptibility. J. J. Thomson[2] first suggested this idea and it was later adopted by Voigt,[3] Langevin,[4] Schrödinger,[5] and H. A. Wilson.[6] The two last named physicists have calculated the value of this susceptibility and find it proportional to the number of free electrons present in unit volume. H. A. Lorentz[7] and van Leeuwen[8] have maintained that free electrons make no resultant contribution to the diamagnetic susceptibility; according to Bohr[9] the diamagnetic effect due to electrons in the interior of the metal is counteracted by the effect of those electrons near the boundary.

The experiments described above are in agreement with the theories of Bohr, Lorentz, and van Leeuwen. Free electrons do not appear to make any contribution to diamagnetic susceptibility. If we assume the change of conductivity of selenium to be due entirely to the freeing of electrons we should expect according to Schrödinger's formula a 35% increase in the diamagnetic susceptibility due to free electrons. Actually no change so large as 0.062% occurred.

Accepting the Bohr-Lorentz-van Leeuwen theories we may also conclude that the electrons which are bound to the molecule in the dark,

[2] J. J. Thomson, Rap. d. Congrès d. phys. Paris, p. 148; 1900.
[3] W. Voigt, Ann. d. Phys., *9*, p. 115; 1902.
[4] P. Langevin, Ann. d. Chim. et d. Phys., *5*, p. 90; 1905.
[5] E. Schrödinger, Wien. Ber., *66*, p. 1305; 1912.
[6] H. A. Wilson, Roy. Soc. Proc. Lond., *97*, p. 321; 1920.
[7] H. A. Lorentz, Vortrage uber die Kinetische Theorie der Materie und der Elektrizität, p. 189; 1914.
[8] Fräulein H. J. van Leeuwen, J. d. Phys., *2*, p. 361; 1921.
[9] N. Bohr, Studier over Metallernes Elektrontheori, p. 106; 1911.

but freed by light, make no contribution to the magnetic effect of the atom to which they are bound,—otherwise their release would alter its magnetic behavior. The diamagnetic susceptibility of selenium must thus be due to electrons confined to the atom, electrons which can take no part in the processes of electric conduction at any time.

From the above-described experiment with silver chloride the conclusion may be drawn that there is no photomagnetic effect in this substance. The discrepancy between this conclusion and Garrison's results may be due to Garrison's failure to eliminate disturbing effects, such as radiometer action or light pressure. On the other hand, the writer examined only one specimen of silver chloride; Garrison tested two different samples and found them to be light sensitive in different degrees. It is possible that some unknown factor operates during the making of the bar to produce photomagnetic sensitivity.

THE RICE INSTITUTE,
HOUSTON, TEXAS.

PHOTO-ELASTIC PROPERTIES OF TRANSPARENT CUBIC CRYSTALS*

By H. B. Maris

ABSTRACT

The photo-elastic coefficients of rock-salt, sylvite and fluorite were measured for the mercury lines 436, 546, and 578 $\mu\mu$ by means of a modified Soleil-Babinet compensator. Compared with glass the coefficient was positive for rock salt, negative for sylvite, positive for fluorite stressed normal to a cube face and negative for fluorite stressed normal to an octahedral face. For all cases, except that of fluorite stressed normal to octahedral faces, relative retardation (Δ) plotted against stress per $cm^2(f)$ gave a straight line for loads between 10 000 and 20 000 gg; this line extended cut the axis of Δ above zero. Therefore for cubic crystals the relation between photo-elastic effects and externally applied force is not the simple direct relation assumed for noncrystalline materials.

When a transparent, optically isotropic substance is put under mechanical stress it becomes doubly refractive. The ratio of the optical change to the change in stress is given numerical magnitude by defining a *photo-elastic coefficient* s. Consider a rectangular bar of the substance subjected to a tension or pressure on the ends and let light be passed through the bar normal to a side of the bar. Let t cm be the thickness of the bar measured in the direction of the light, f the force per unit cross section of the bar, and Δ the optical path difference for beam polarized respectively parallel and normal to the length of the bar. Then s is defined by the relation:

$$s = \partial\Delta / t\partial f \qquad (1)$$

Δ and hence s is a function of the wave length of the light.

Early measurements of the photo-elastic coefficients of the cubic crystals, rock-salt, sylvite, and fluorite were made by Pockel.[1] The values were given only for sodium light and for a limited range of pressures. In this paper are described measurements by an improved method of the photo-elastic coefficients of these same crystals for three wave lengths of lights in the visible spectrum. The lines 436, 546, and 578$\mu\mu$ of the mercury arc were used, separated by suitable color filters. In some cases better measurements were made by observing the colors through a diffraction grating. The double refraction at any desired point in the crystal was measured by means of a calibrated quartz com-

* Released for publication by the Navy Department.

[1] Pockel, Ann. d. Phys., *39*, p. 440; 1890.

pensator,[2] consisting of two thin quartz wedges with the optic axes in the respective wedges at right angles. When the field seen in the analysing Nicol was made dark by the compensator, Δ could be determined directly from the thickness of the compensating plate of quartz.

Crystals with faces ground plane parallel were placed in the loading frame as shown in Fig. 1. By means of the plumb-bob *D* the center of the crystal was placed directly below the knife edge *E*. The load was applied by the spring balance *G* through the lever arm *F*. The crystal

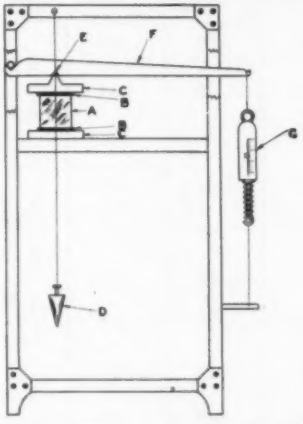

FIG. 1. *Loading frame: A crystal with plane parallel faces; B blotting paper pads; C steel loading plates with polished plane faces; D plumb-bob for lining the knife edge, E with the center of the crystal; F lever arm; G spring balance.*

was protected from excessive stresses near the edges due to unequal expansion between the crystal and the loading plates *CC* by two pads of blotting paper *BB*. In spite of these pads the stress distribution was not uniform throughout the crystal but was high near the edges in contact with the pads, however, the center of the crystal as viewed through the centers of two opposite faces presented a uniform field and in each of the experiments all readings were made at some point near the center of the crystal. In this way it is felt that errors due to lack of uniformity of stress in the crystal were kept below 1%.

Each crystal studied showed some initial or residual double refraction which was irregularly distributed throughout the crystal and as a rule was not quite the same at the beginning and end of the experiment.

[2] Drude, Theory of Optics, p. 258; 1925.

With each crystal some point near the center where this residual double refraction was zero was selected all readings were then made on this point, thus avoiding errors due to the lack of symmetry in the crystal.

TABLE 1. *Photo-elastic coefficient for NaCl, Crystal 2*

1	2	3	4	5	6	7
Stress in grams per sq. cm, f	Relative retardation in wave lengths, Δ			Photo-elastic coefficient, $s \cdot 10^6$		
	$\lambda=436$	$\lambda=546$	$\lambda=578$	$\lambda=436$	$\lambda=546$	$\lambda=578$
0000	.025	.023	.019			
				9.08	6.84	6.04
1950	.139	.108	.104			
				10.6	8.23	7.38
3250	.227	.176	.165			
				7.03	5.58	5.33
4550	.285	.222	.209			
				4.00	3.15	3.03
5850	.318	.248	.234			
				4.28	3.29	3.07
7870	.378	.294	.277			
				4.68	3.67	3.44
10530	.457	.356	.335			
				5.04	3.95	3.78
13000	.536	.418	.394			
				5.33	4.06	3.82
15600	.624	.485	.457			
				5.27	4.18	3.85
18200	.710	.554	.520			
				2.14	1.65	1.57
24000	.789	.615	.578			
				2.90	2.32	2.17
15600	.630	.491	.462			
				6.38	4.94	4.67
10340	.417	.326	.306			
				7.00	5.49	5.14
5850	.199	.155	.146			
				5.08	3.96	3.71
1950	.073	0.57	.053			
				7.6	5.84	5.52
000	−.02	−.016	−.015			

In Table 1 are given the measurements, in the order in which they were taken, for a crystal of rock-salt 6.35×6.35×5.00 cm with natural faces compressed normally to the largest face and traversed by plane polarized light in the directions of the longest edge. Column 1 gives the

load f on the crystal in grams per sq. cm. Columns 2, 3, and 4 give Δ in wave lengths for the blue, green and yellow lines, respectively. columns 5, 6, and 7 were calculated by means of (1).

The measurements of column 2 are plotted as ordinate against f as abscissa in curve 1, Fig. 2. The photo-elastic coefficient s is determined from the slope of the curve at each point and is given in column 5, Table 1. It is seen that s for small loads decreased with increase of the stress until a load of 5 000 grams per sq. cm was reached. It was then quite uniform until the load exceeded 20 000 grams where there occurred an additional drop in the value of s due probably to plastic deformation.

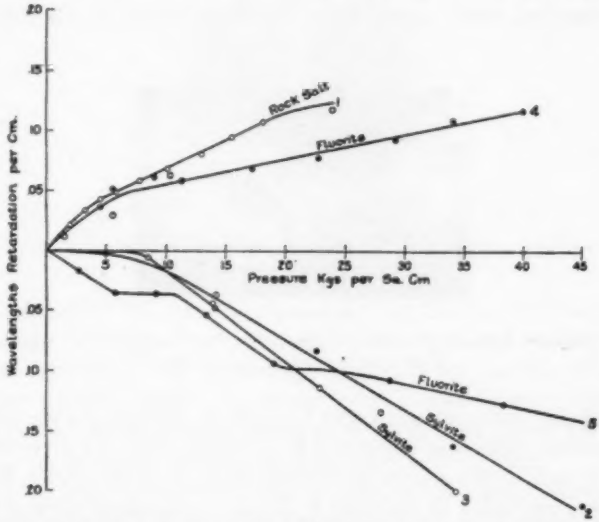

FIG. 2. *Double refraction of the mercury blue line λ 436 versus stress for cubic crystals. The slope of the curve for a given load defines the photo-elastic coefficient (s) of the crystal for that load.*

This is opposite to the case of stretched celluloid where plastic deformation increases the double refraction. Values of s obtained with increasing load are much more uniform than those measured with decreasing load. This was probably due to a hysteresis in the photo-elastic effect.

A second crystal of rock salt $7.88 \times 4.37 \times 2.84$ cm, also with natural faces, gave, within the error of experiment, the same relation between stress and double refraction as curve 1, Fig. 2. When it was subjected to a load of 31 500 grams per sq. cm, slip planes or planes of failure appeared making an angle of about 45° with the direction of the load.

The planes which persisted after the load was removed, are shown in Fig. 3. They appeared as sharp bright lines when the unstressed specimen was viewed in plane polarized light with the plane of polarization parallel to a face of the crystal, but when the plane of polarization was parallel to the lines they could not be seen. This meant that the slip planes of plastic deformation were planes of double refractive material with the optic axis in the plane of the deformation. This is in agreement with the recent observations of Obreimow and Schubinkoff.[3] In passing it is of interest to point out that a similar slip plane phenomenon was observed in the case of overstrained celluloid. The lines are clearly seen in the photograph of Fig. 4. In this case the planes of deformation were perpendicular to the direction of the deforming force.

FIG. 3. *Slip planes in an over strained rock-salt crystal. Photographed in horizontally polarized light, after the load had been removed.*

A rock salt cube was subjected to pressure normal to two 110 faces and a second cube was compressed normal to two 111 or octahedral faces. In each of these cases the relation between double refraction and stress was the same as that for a crystal compressed normal to the natural or cube faces.

Two crystals of sylvite with natural cubic face were studied. The measurements made with the first crystal of dimensions $3.05 \times 1.46 \times 1.0$ cm are plotted in curve 2, Fig. 2 and those for the second crystal, $2.54 \times 1.06 \times .558$ cm in curve 3. The double refraction for sylvite was negative to that of rock-salt.

A crystal of fluorite $3.55 \times 3.05 \times 1.60$ was compressed normal to a cube face and gave the retardation plotted in curve 4. A second flat crystal with two octahedral faces 10.06 cm^2 in area was stressed normal to these faces. The light path through the crystal was 3.885 cm and the

[3] I. W. Obreimow and L. W. Schubnikoff, ZS. f. Physik, *41*, p. 907; 1927.

thickness was 1.18 cm. The measurements made with this crystal were very irregular. Changes due to plastic deformation seemed to be large and it was very difficult to repeat readings with satisfactory accuracy.

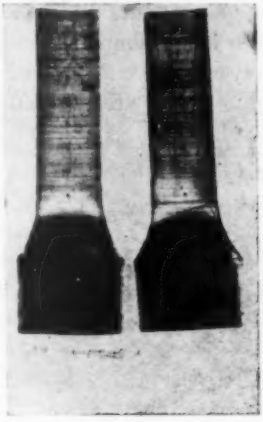

FIG. 4. *Slip planes in an over-strained strip of celluloid. Photographed in circularly polarized light after the load had been removed.*

The irregularities of curve 5 represent irregularities observed in the relation between double refraction and stress. Repeatedly large changes of stress resulted in no observable change in the double refraction. Often the stress was shifted back and forth several times between two limiting values with no change being shown in the refraction, but a slight change beyond either limit resulted in a measurable effect.

It is interesting to note that all of these curves except curve 5, are concave downward. Table 2 gives average values for s calculated from all of the measurements made. Columns II, III, and IV give values

TABLE 2

I	II	III	IV	V
	$\lambda=436$ $s\cdot10^6$	$\lambda=546$ $s\cdot10^6$	$\lambda=578$ $s\cdot10^6$	$\lambda=589$ $s\cdot10^6$
NaCl	5.04	3.77	3.32	3.73
KCl	−6.82	−5.31	−5.00	−4.71
CaF_2 cubic	3.96	3.08	2.90	3.56
CaF_2 octahedral	−4.29	−3.34	−3.14	

obtained by the author with the mercury blue, green, and yellow lines and Column V gives values for s given by Pockels for the sodium yellow line.

For noncrystalline bodies strained within the elastic limit, the relation between externally applied stress and the accompanying photo-elastic effect is a simple proportionality. These studies show that for cubic crystals the relation is not simple, since the sign of the effect is not the same for all crystals and no crystal showed a direct proportionality between photo-elastic effect and stress for all stresses below the elastic limit.

NAVAL RESEARCH LABORATORY,
WASHINGTON, D. C.
JUNE, 1927.

Molecular Spectra in Gases. (Bulletin No. 57 of the National Research Council). By E. C. Kemble (Chairman), R. T. Birge, W. F. Colby, F. W. Loomis, and L. Page. 358 pages. National Research Council, Washington. $4.00. Bound, $4.50.

Physicists interested in band spectra have long been eagerly awaiting the publication of this bulletin, which constitutes the report of the National Research Council Committee on Radiation in Gases, and its final appearance gives full warrant for their high expectations. Dozens of books of varying quality have been written on "atomic structure and spectral lines," but the literature has been singularly free from adequate treatises on band spectra, which belong to molecules rather than atoms. Consequently the appearance of an authentic monograph on recent developments in this subject fulfills a real need, and Prof. Kemble and his committee are to be congratulated on achievement of a difficult task.

Chapter I, by Kemble, is a brief and lucid introduction, written especially from the historical standpoint. Chapter II, by Page, is a thirty-page survey of "quantum dynamics and the correspondence principle," but entirely on the basis of the old quantum theory rather than the Heisenberg-Schroedinger mechanics, which were developed too late for incorporation. Chapter III, by Colby, is on "infrared absorption bands," and fits closely with Chapter I. It gives a clear, easily followed descriptive account of experimental work and elementary theory in the infrared.

The infrared absorption bands studied in Chapters I and III are the simplest and best-known examples of molecular spectra, but undoubtedly the most prolific variety are the "electronic bands," which are emitted when there are changes in the quantum numbers of the electrons, simultaneously with alterations in the rotational and vibrational quantum numbers of the nuclei. Chapter IV, very appropriately written by Birge, is devoted to this important, rapidly growing subject of electronic bands, and constitutes over one-half the bulletin. The content includes a wide range of phenomena, such as the puzzling doublet levels, the complicated intensity distributions in vibrational sequences, and the recent rather spectacular spectroscopic derivations of heats of dissociation. A wealth of detail is given, and the analysis of the literature is scholarly and comprehensive. Certain portions of the chapter, such as the discussion of combination relations and the very necessary numerical work of adjusting constants to fit experimental data, are rather technical and indigestible for the casual reader, although important to the specialist. Possibly this material might have been reserved for an appendix or otherwise set aside from the more descriptive passages. The table of constants of molecules compiled by Prof. Birge on pp. 230–232 is a real, much-needed contribution to the tabular data of modern physics, and its possession will be indispensable to all students of molecular structure.

Chapters V and VI, by Loomis, are devoted respectively to the isotope effect (spectroscopic detection of isotopes) and to fluorescent band spectra, and are both good accounts of interesting subjects. The concluding chapter, by Kemble, is on "molecular models and related topics," and contains considerable original work which he has not published elsewhere. Throughout much of the bulletin rather too much credence, in our opinion, is given to the rigid Kratzer-Kramers-Pauli model involving simultaneous stationary components $\sigma h/2\pi$ and $\epsilon h/2\pi$ of electronic angular momentum parallel and perpendicular to the molecular axis. Consequently it is gratifying to see some discussion in the final chapter of the serious dynamical objections to this model. In sections 3 and 4 of his chapter Prof. Kemble reaches independently by a different method the same conclusion as Miss Mensing that σ and ϵ cannot be simultaneously different from zero. In the next section he gives a very useful summary of an important paper by Hund which applies to band spectra the concept of an electron spin previously so useful in the study of atomic spectral lines. Hund's ideas seem to furnish the clue to the adequate interpretation of many phenomena in molecular spectra, and it is unfortunate that his paper did not appear early enough to be usable as a focal point for the discussion in earlier chapters. In particular, more stress would be advantageous on the fact that an apparent Kratzer ϵ is often in reality probably due to loose coupling of the electron's spin axis (Hund's coupling of type b). Prof. Kemble closes with an excellent discussion of the Zeeman effect in band spectra, an interesting and complicated subject on which the literature has previously been inadequate.

We have already intimated that the book was written at a difficult time, during the period of transition from the old to the new quantum mechanics and to the spin electron, but at the same time we must emphasize that the bulk of the material (such as descriptions of experimental work, empirical formulas, etc.) is of such a character as not to be altered in essential nature by the new developments. The plan of having individual chapters written by different committee members who are experts in the particular fields involved has the advantage of making the bulletin thoroughly authentic, but involves a certain amount of duplication and unevenness of style, especially as regards fullness of detail. The notation and terminology, however, have been kept scrupulously uniform, and a useful syllabus of this is given at the beginning of the book. The documentation of references to the literature is very complete throughout. It seems unfortunate that so important a book contains neither a subject nor an author index. On the other hand it is comforting that at last a physical bulletin of the National Research Council is available with a cloth rather than paper cover. and is printed on paper of better quality.

J. H. VAN VLECK

INSTRUMENT SECTION

PHOTO-ELASTIC INVESTIGATIONS OF THE TENSIL TEST SPECIMEN, THE NOTCHED BAR, THE SHIP PROPELLER STRUT, AND THE ROLLER PATH RING*

By H. B. Maris

INTRODUCTION

During the past two years photo-elastic investigations, i.e., the analysis of stresses in a specimen by means of polarized light transmitted through the specimen, have been carried out by the author under the direction of Dr. E. O. Hulburt. The present paper describes the the methods of photo-elastic analysis, including new ways of measuring both the double refraction and the deformation resulting from stress. The results of investigations of the tensil test specimen, the notched bar, the ship propeller strut and the roller path ring are given. In each case new, although not unexpected, facts concerning strain members have been brought out very simply by the experimental photo-elastic method, facts which would be difficult of discovery by a direct mathematical analysis.

EXPERIMENTAL METHODS

The technique of photo-elastic research consists simply of methods for accurately measuring the direction and magnitude of the load applied to the test member being studied, methods for measuring the magnitude and direction of the resulting double refraction in different parts of the test member and determination of the converting factor for the relation between double refraction and value of the stress difference $(P-Q)$ in the specimen.

The solution of a photo-elastic problem is based on the assumption that for the material used and under the conditions of the experiment, a direct proportionality exists between the stress per unit area, the deformation per unit length in the direction of the stress and the double refraction per unit thickness perpendicular to the direction of the stress. If this assumption is correct, the direction of the optical axis of double refraction at a specified point in a stress member gives the direction of the P or Q stress known as the principal stress,[1] at the point. Furthermore, a measurement of the magnitude of the double refraction gives, upon multiplication by the correct converting factor, the value of $P-Q$ at the point. Thus $(P-Q)$ at each point in a test specimen is determined by measuring the resulting double refraction, $P+Q$ may be determined by calculation or by a separate experiment, then P and Q

* Released for publication by the Navy Department.

[1] A. E. H. Love, Mathematical Theory of Elasticity, Chapter 1, 1906.

separately are known for all points of the specimen. The assumption has been justified by the investigations of J. Kerr,[2] Cyrus Wilson,[3] L. N. G. Filon,[4] M. M. Mesnager,[5] and E. G. Coker,[6] who found no case where an isotropic medium under deformation within the elastic limit of the material failed to show a double refraction which was proportional to the deformation. In general, photo-elastic studies of stresses are limited to elastic materials which will transmit light, to test members with plane parallel faces and to problems of stresses in one plane. The results obtained from a test of a member are applicable to all geometrically similar members made of elastic material and stressed within the elastic limit, i.e., where Hooke's law holds. The results may be extended, however, to yield conclusions concerning stresses of inelastic material and material stresses beyond the elastic limit. Problems involving stresses in three dimensions can only be studied when they can be reduced to a combination of two or more problems of stresses in a plane.

The state of stress at a point in a strained medium is represented by the "strain ellipsoid" at the point. The magnitude and the direction of the axes of the ellipsoid are the magnitude and direction of the "principle stress known as the P, Q, and R stress. Since the photo-elastic method is essentially one of two dimensional analysis, there are only two principal stress, P and Q, which are mutually perpendicular, to be considered, and the method is simply a means of measuring P and Q at each and every point of the medium.

Any isotropic medium under strain becomes double refractive with the result that in general the light passing through the medium will be separated into two rays. In two cases, however, the light is unchanged; namely, when the plane of vibration of the light is parallel or perpendicular to the direction of the principal strain. When the plane of vibration is at any other angle a separation into two different rays occurs. The ray vibrating in the direction of the P stress is retarded or advanced an amount which is directly proportional to the value of the P stress (compression or tension) at that point. On the other hand the beam vibrating in the direction of the Q stress is retarded or advanced an amount which is proportional to the compression or tension of the Q stress. The net result of both actions is then a double refraction at

[2] J. Kerr, Phil. Mag., *26*, p. 321; 1888.
[3] Cyrus Wilson, Phil. Mag., *32*, p. 481; 1891.
[4] L. N. G. Filon, Pro. Roy. Soc., *223*, p. 89; 1923.
[5] M. Mesnager, Annales des Ponts et Chausses, 4 ser. 9t, *16*, p. 135; 1913.
[6] E. G. Coker, B. A. Rept., *92*, p. 313; 1924.

the given point which is proportional to the difference between the principal stressed $(P-Q)$ at that point.

When the specimen is observed between crossed nicol prisms, interference colors similar to those seen in a thin sheet of mica observed between the nicols are seen. Just as the mica will appear black, independent of the thickness, when its optic axis is parallel to the axis of either nicol, so the stress specimen will appear black at all points where the direction of the stresses coincide with the direction of the optic axis of the nicols. Thus, when the nicols are set at some given angle with reference to a fiducial reference line of the stress member the part of the specimen which appears black is the locus of those points at which the strain lines make the given angle with the reference line. When the direction of the stress is kept constant, while the crossed nicols are set at different angles, regions of constant slope or "isoclinic" lines can be drawn on an image of the specimen which show the direction of the stress lines for all parts of the specimen. Isoclinic lines for the stresses surrounding the base of a notch in a beam clamped at one end and bent by a torque about the other end are shown in the photographs of Fig. 9 where *B* shows the 80 degree and *C* the 30 degree isoclinic. Complete maps are shown in Fig. 11. From these isoclinic lines the strain lines (see Fig. 12) were plotted. The strain lines are the lines whose direction at each point is the direction of the principal strain at that point. The P and Q strain lines compose two families of mutually orthogonal curves.

By the use of circularly polarized light and the measurement of interference colors, values of $P-Q$ are obtained at every point of the specimen. The lines of equal color, which represent $P-Q$ a constant are called the isochromatic lines or "isochromatics." Fig. 9 *D*, *E*, and *F* show typical sets of isochromatic lines where $P-Q$ is zero at the line 0 and increases toward the line 3. Fig. 10 shows isochromatic maps of the notched bar.

Thus far we have described how the directions of the strains and the values of $P-Q$ are determined. In order to determine P and Q separately two methods are available, one by direct calculation from the isoclinics and the isochromatics and the other by a separate experiment.

In the first method, the one of the direct calculation, which is due to L. N. G. Filon, the values of P and Q are calculated from the equations:

$$P = P_0 + \int_{\phi_0}^{\phi} (P-Q) \cot \Psi \, d\phi \qquad (1)$$

$$Q=Q_0+\int_{\phi_0}^{\phi}(Q-P)\cot\Psi_1\,d\phi \tag{2}$$

$$P=P_0-\Delta\int_0^A\frac{P-Q}{\Delta y}ds \tag{3}$$

In the above equations ψ is the angle through which a line of stress must be rotated counter-clockwise to make it coincide with an isoclinic. ψ_1 is obtained from ψ by rotation of 90°. ϕ is the angle which the lines of of stress make with some reference line in the specimen. The right hand members of these equations may be integrated geometrically. Equations 1 and 2 cannot be used for values of ψ near 0°, 90°, or 180°, for those conditions equation III must be used. A detailed discussion of the method of integration is given in Filon's paper.[7]

The above equations are approximate solutions of the stress integration problem based on the assumption that the change in the radius of curvature of the stress lines is small compared to the distance measured along the lines of integration. This is, in general, true, but where studies of stress are made in the neighborhood of a crack or a sharp notch this assumption is not valid and the equation from which Filon obtained equations 1, 2 and 3 must be used.

$$dP/dS+(P-Q)/r'=0 \tag{4}$$

where dP is the change in the P stress over a distance dS along the direction of that stress and r' is the radius of curvature of the Q stress line at the given point. Solving for dP we have:

$$dP=(Q-P)ds/r' \tag{5}$$

$$dQ=(P-Q)ds/r'' \tag{6}$$

These equations may be solved by a geometric integration along any of the P or Q lines. The value of $1/r$ was obtained at different points by matching the curvature of the stress line with a curve calibrated to give direct values of $1/r$, or by calculation, from the usual equation

$$1/r=\phi/\text{arc} \tag{7}$$

where ϕ is the angle which separates two near isoclinic lines, and the arc is approximately equal to the distance between two near isoclinics measured perpendicular to the stress line. For an integration of equation 5 along line 7, Fig. 12 see Table 1 and Figure 14. Fig. 12 shows the P and Q stress lines in an Izod notched bar clamped at *cc* supported

[7] L. N. G. Filon, B. A. Report, *93*, p. 351; 1923.

at b and loaded at a. Fig. 14 shows the values of $(P-Q)1/r$ for points along Line 7 plotted as ordinate against distance along the line (d) as abcissa. The area under the curve between any two values of s is equal to the change in P stress between the two points. The results are entirely independent of the scale of the map since a change in r is canceled by a similar change in ds. The integration can generally start at a boundary where the normal stress is 0 and the tangential stress is equal to $(P-Q)$.

Table I shows calculations for the integration along the line. Column 1 gives distance along the line in inches. Col. 2 gives the value of $Q-P$ in pounds per square inch. Column 3 gives the value of $Q-P/r$ at the given point. Column 4 gives the change in P between two adjacent points. This figure is obtained as the area under the integration curve of Fig. 14. The figures of the fifth column are obtained by adding the opposite figure in the fourth column to the preceding figure in the fifth column. Since errors are carried along by this method it is always best to integrate from the smaller to the larger values of the stress. the figures of column 6 are obtained by the addition of a figure in column 5 to the corresponding figure in column 2. The figures of column 7 are then obtained by the addition of corresponding figures in column 5 and 6.

Line 7 was chosen to demonstrate the method of the integration because of the varying conditions found along the line. At the point a $S=0$, $P=\infty$; therefore it is not possible to start integration from that point. Near the point $S=1.0$ Line 7 is crossed by another line of integration and we are able to take the values of P and Q from that point. We have therefore integrated in both directions from the point $S=1.0$. Near the point $S=2.8$ the values of $Q-P$ are very large and at the same place the value of $1/r$ is indeterminate; therefore we cannot integrate past this point but drop the integration here and start from the other end of the line at the point $S=6.8$ where $P=Q=0$ and work back to the point $S=2.9$.

The second method, the one requiring a separate experiment, has been used extensively by E. G. Coker.[6] This method involved the determination of $P+Q$, by the measurement of the change in thickness of the test piece, which is proportional to $P+Q$. The direct measurements made with an extensometer, after the manner of Coker, were found to be difficult; first, because the limiting errors of the measurement were great; second, irregularities in the surface of the pyralin introduced

TABLE 1. *Integration for line 7, Fig. 14.*

1	2	3	4	5	6	7
S inches	$Q-P$ pounds per. sq. inch	$\frac{Q-P}{r}$	dF pounds per. sq. inch	P pounds per. sq. inch	Q pounds per. sq. inch	$P+Q$ pounds per. sq. inch
.1	350			−220.9	129.1	− 91.8
.2	130	− 481	−134.4	− 86.5	43.5	− 43.0
.4	70	− 126	− 51.0	− 35.5	34.5	− 1.0
.6	35	− 43.0	− 15.7	− 19.8	15.2	− 4.6
.7	30	− 3.9	− 1.9	− 17.9	12.1	− 5.8
.8	25	37.5	1.5	− 19.4	5.6	− 13.8
1.0	30	57	8.4	− 27.8	2.2	− 25.6
1.2	55	126.5	− 18.3	− 46.1	8.9	− 37.2
1.4	80	184	− 32.9	− 79.0	1.0	− 78.0
1.6	140	252	− 47.0	−126.0	14.0	− 112.0
1.8	180	254	− 49.6	−175.6	4.4	− 171.2
2.0	310	465	− 68.8	−244.4	65.6	− 178.8
2.2	440	513	−118.5	−362.9	77.1	− 285.8
2.4	550	1045	−176.2	−539.1	10.9	− 528.2
2.6	716	1061	−253.2	−792.3	− 76.3	− 868.6
2.7	950	2185	−187.4	−979.7	− 29.7	−1009.4
2.8	2000	20.000				
2.85	2000	34.000				
2.92	730	3650				
3.2	560	728	−117.	−498	62.	− 436.
3.4	460	460	− 87.	−381.	79.	− 302.
3.6	400	− 360	− 57.	−294.	106.	− 188.
3.8	270	− 343	− 41.	−237.	33.	− 204.
4.0	170	− 153	− 30.	−196.	− 26.	− 222.
4.2	147	− 132	− 76.	−166.	− 19.	− 195.
5.0	100	− 100	− 90.	− 90.	10.	− 80.
6.8	00	0	00	00	00	00

errors which were great; and finally, the point measured could not be located on the test piece with accuracy at places where the change in the stresses was great. An optical method was developed in this laboratory in which the measurement of the change in thickness was made by

passing monochromatic light through the optical system outline in Fig. 2 and counting the movement of interference fringes with the changing distance between the test piece *e* and the glass plate *d*. This method in itself leads directly to extremely accurate measurements, consequently effects resulting from distortion of the relation between the surfaces of *e* and *d* are very important.

The method was developed with special care as to the means of detecting and avoiding errors. The test member *e* was clamped between two glass plates *dd* which were held in firm contact with the member at one end while the other ends were held apart by spacers which left the member free to expand and contract, but prevented any bowing or distortion of the plates when the member was stressed. Monochromatic light from *a*, focused by the lens *b*, reflected by the glass plate *c* and observed through the lens *f*, gave interference fringes between the surface of the glass and the adjacent surface of the member. This is an extremely delicate and accurate method of measuring small displacements since direct measurements were easily made to 0.00001 in. By arranging the member so that observations could be made on first one side and then the other, without disturbing the relation between the member and the plates, errors due to warping of the member under stress were eliminated. Errors due to friction between the member and the plates appeared as an irregularity in the movement of fringes past a point with increasing stress and were easily detected and eliminated. The great advantage of this method besides its accuracy is that it presents to the eye at one time a picture of the relative changes in the entire field. The reduction of this picture, however, to a cross checked diagram of stresses in the member with allowances for warp in the member and in the glass plate, for change in the separation of the plates and other errors, was such a laborious task the optical method was used only as a check on the results obtained from the method of calculation except for studies of stresses at the base of a sharp notch where the optical method was used in all measurements.

A diagram of the apparatus used in making the photo-elastic studies is shown in Fig. 1. A 1000 watt moving picture globe *a* inclosed in a 40″x20″x20″ house *b*, was used as a source of light. A water cooling cell *d* was introduced between the source of light and the first nicol prism *f* to protect it from excessive heat. A large lens *c* with a short focus was needed as a condenser; this gave a strongly converging ray which could not be passed through the nicol prism, therefore the diverging lens *e* was

inserted to give a nearly parallel beam through the nicol which was placed at the point of focus of the beam. The beam, which had been plane polarized by the nicol *f*, was circularly polarized on passing through the quarter wave plate *g* and diverged to fill the entire field of lens *h* which was focused to give parallel rays. This path of parallel rays was the field in which the test piece was placed. The beam of light after passing the testing frame *i* fell on a second large lens *j*, the weakly

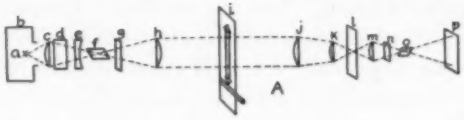

FIG. 1. *Arrangement of optical apparatus for photo-elastic studies.*

converging beam from *j* fell on the short focus lens *k*, and an image of the test member was formed at *l* where a comparison member was placed in the same plane with the image in order that lens *m* might

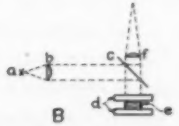

FIG. 2. *Interference method of measuring very small changes of thickness.*

project both on the screen *p*. The circularly polarized beam then passes through a second quarter wave plate *n* and was plane polarized in the original plane of nicol *f* when there was no other doubly refractive material in the path of the beam. The plane polarized beam then passes into nicol *o* which was set for extinction and all of the beam was absorbed. When the test members at *i* and *l* were stressed the polarization of the light passing through them was changed as eliptically polarized light changes when it passes from circular polarization at 0° to plane polarization at 45° through circular polarization again at 90° and is again plane polarized at 135°. The change was directly proportional to the stress and varied with the wave length, being greater for the short waves. The light falling on nicol *o* then was not all in the plane of nicol *f* and part of it was transmitted. The color transmitted depended on the amount of rotation and consequently the color of a point on the image was a measure of the stress differences $(P-Q)$ at the corresponding point on the stress member. The lines of equal color were marked on the image of the test member on ground glass (see *E*

and *F* Fig. 9 and *A* and *B*, Fig. 10). The different colors were calibrated for values of $(P-Q)$ by measuring the stress needed to produce the same color in a uniform comparison bar of the same material and of the same thickness.

There are, however, several disadvantages to the use of interference colors and a comparison bar for determining values of $P-Q$. It is very difficult to standardize shades of color so that a given shade will always represent a definite double refraction. It is also very difficult to compare different colors or shades seen at different times and under different intensity of light, and finally, the colors of the image do not always give

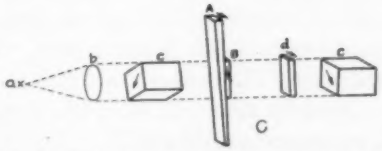

FIG. 3. *Soleil-Babinet type of compensator for measuring double-refraction.*

sharp contrasts which will allow a close evaluation of $P-Q$. These difficulties have been avoided by the use of a specially constructed compensator of quartz.

The optical effects of stress in an isotropic medium on monochromatic polarized light passing through it is exactly the same as that of a thin plate of quartz in the path of the beam if the thickness of the quartz plate is everywhere proportional to the magnitude of $P-Q$ and the direction of the optical axis of the crystal is everywhere parallel to the greater stress for compression and to the smaller stress for tension. If now this imaginary quartz plate be rotated about the beam of light as an axis through an angle of 90° its double refraction will cancel that of the stressed member and show a dark field through the second Nicol. A compensator giving the optical effect of a quartz plate of variable thickness is shown in Fig. 3. It consists of two quartz wedges *A* and *B*, with optical axes as shown by the arrows. The edges of wedges *B* are slightly over one inch in length, then as the slopes of wedges *A* and *B* are identical the compensator will present in polarized light a uniform field over the entire opening. Wedge *A* is moved along under *B* by means of the ratchet, the magnitude of the movement is read on a vernier. If the compensator is placed perpendicular to the path of a polarized beam of light between the crossed nicols *CC* rotation of the compensator about an axis parallel to the beam and movement of the

wedge *A* across the field will completely compensate any double refraction which may result from a doubly refractive medium at *d* for any particular wave length desired. The compensator as constructed in this Laboratory has in the wedge *A* a difference in thickness of the two ends of one-twentieth of an inch, and gives a relative retardation of about 15 wave lengths in the red and 25 in the blue of the extraordinary ray over the ordinary ray.

The use of such a compensator in the photo-elastic studies has made it possible to measure double refraction in terms of wave lengths and fractions of wave lengths retardation with monochromatic light. It is thus possible to establish and compare standards with far greater accuracy than could be possible under a system which depended upon a comparison of shades of color in a fringe system. Measurements can be made by compensating the double refraction to extinction or by compensation to a sensitive tint. .01 wave length retardation can be measured without additional equipment.

TABLE 2. *Photo-elastic stress standards for pyralin.*

1 Tension per sq. in.	2 Color of bar	3 Compensator reading for λ436	4 Retardation for λ= .436
0000	black	.03	.015
200	grey-muddy	.40	.265
400	white	.79	.524
600	light lemon	1.18	.782
800	dark orange	1.52	1.008
1000	plum	1.97	1.308
1200	sky blue	2.40	1.590
1400	pea green	1.75	1.823
1600	lemon	3.14	2.080
1800	tangerine	3.57	2.365
2000	plum	3.93	2.600
2400	pea green	4.83	3.180

Table 2 gives color compensator standards for the relation between double refraction and stress in a stretched bar of celluloid 1/4″ thick. Column 1 gives tension per sq. in., column 2 the observed color, column 3 the compensator reading, and column 4 the relative retardation for the mercury blue line λ436. Double refraction is proportional to the stress from 0. to 2000 pounds per square inch; at 2400 pounds per square inch the double refraction is 2% higher than the photo-elastic ratio

would indicate it should be. The specimen showed an initial double refraction which measured .015 on the compensator.

The one objection to the use of a quartz compensator in place of comparison bar of stretched celluloid in studying photo-elastic effects in celluloid, is that dispersion may not be the same for quartz and stressed celluloid. This difference was hardly measurable in the above experiment

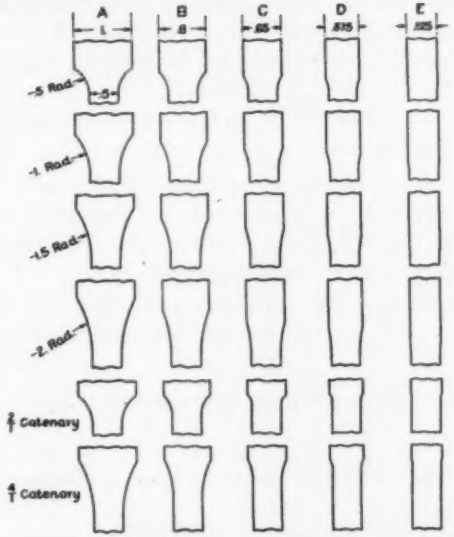

FIG. 4. *Curved part of "shoulders" of tensil test specimens studied.*

and the one advantage of the quartz is that both the dispersion and double refraction are fixed and are not changed with time, while in a comparison strip of celluloid both dispersion and double refraction do change with time. The dispersion is especially subject to errors due to plastic deformation. The quartz compensator was, on the whole, a more satisfactory method of measuring double refraction than the comparison strip.

STRESSES IN FLAT TENSIL TEST SPECIMENS

A study was made of a series of flat tensil test specimens of uniform dimensions in the neck but with differing width and curvature for the shoulder (see Fig. 4). Fig. 5 shows in detail the notation used to designate the different dimensions and points of special interest of the specimen. It is self explanatory except for the dotted curves NyN and

NzN and the two points *m*. When the specimen was under tension in the photo-elastic apparatus the intrusion of the stresses due to the shoulders into the narrow part could be seen to fade out along the curve NzN. NzN then, marks the limit of the observable effect of the shoulders upon the narrow part. No measurements of the stresses along the curve NzN could be made which means that the change in $P-Q$ from the value along B was less than 2%. It was only by going back to the curve NyN

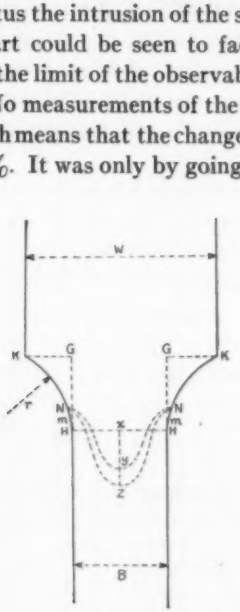

FIG. 5. *Plan of the "shoulder" of a tensil test specimen.*

that the stresses had changed a measurable amount. The actual change in the $P-Q$ values from the region NzN to NyN was about 6% of the value along B. The length of the line XZ is a measure of the intrusion of 2% changes in the stresses into the narrow part of the specimen and the line XY shows the distance 6% of changes of stresses from the shoulders extended into the narrow part. The two points *m* of Fig. 5 are the region of maximum tension. These points varied but slightly in location in the different specimens, but were invariably above the line HH or limit of minimum section area. The points "*m*" exist only when there is an increase in tension above that of the minimum section. In Table 5 specimens showing a maximum stress of 1000 lbs. per square inch have no point *m*.

Three questions are answered regarding each of the specimens shown in Fig. 4.

(1) At what distance below the line HH Fig. 5 are changes in Stress due to the shoulders KK less than 2% of the value of $P-Q$ at B?

(2) At what distance below the line HH Fig. 5 are changes of 6% in stress due to the shoulders KK present?

(3) What and where is the maximum tension in each specimen when the average tension in the narrow part of the specimen is 1000 lbs. per square inch?

The answer to the first of these questions is given in Table 3 and the solid lines of Fig. 6. The answer to the second question is given in Table 4 and the broken lines of Fig. 6. The answer to the third question is given in Table 5. A detailed description of the Tables and Figures follows.

Fig. 4 shows the curved parts HK (Fig. 5) of each of the specimens studied. All the specimens have the same width of the narrow part, .5 inch; they have different widths W of the shoulders and different curvatures from the shoulders to the narrow part. The specimens of each row of Fig. 4 have the same curvature for the arc HK (Fig. 5) but different widths W. The specimens of each column of Fig. 4 have the same width W, but different curvatures. The curvatures of the arcs HK for the different rows of Fig. 4 are as follows:

Row	Curvature
1	arc of a circle of radius 1/2 inches
2	" " " " " " 1 inch
3	" " " " " " 1 1/2 inches
4	" " " " " " 2 "
5	" " " Catenary ratio 2/1 (GH/CK Fig. 5)
6	" " " " " 4/1 "

The values of W for the different columns of Fig. 4 are as follows:

Column	*W in inches*
A	1.
B	.8
C	.65
D	.575
E	.525

The letter of the column and the number for the row of a specimen in Fig 4 is a complete identification of the dimensions of the specimen; for illustration, $C-1\ 1/2$ means the specimen for which $W=0.65$ inches and the curve HK is the arc of a circle of radius 1 1/2 inches.

Table 3 gives the maximum observed distance of intrusion of stresses in to the parallel part of the specimen represented by the length of the line XZ, Fig. 5. This table shows that the line XZ does not always de-

crease with decreasing values for w. For example with the catenary of ratio 2/1 ("2-Cat" of Fig. 4 and Table 3) there is a noticeable increase in XZ with a decrease in W. The data of Table 3 are plotted in the solid

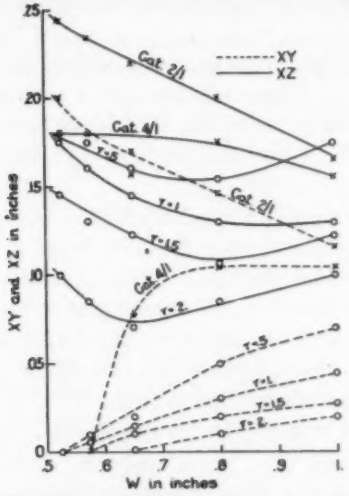

FIG. 6. *Thickness of "shoulder" (w) plotted against extension of stress into the parallel part or "neck" of the specimen.*

line curves of Fig. 6 where the length XZ is plotted as the ordinate against W as abscissa. These curves show at once that XZ does not in general increase with increase of W.

TABLE 3. *Maximum observed intrusion of shoulder stresses into the parallel part of the specimen, represented by the line XZ, Fig. 5.*

1	2	3	4	5	6
		Intrusions at various widths of W			
Curvature	A 1.0	B .80	C .65	D .575	E .525
1/2	.175	.165	.160	.175	.175
1	.130	.130	.145	.160	.175
1−1/2	.122	.117	.122	.130	.145
2-Cat	.168	.210	.220	.235	.245
4-Cat	.156	.172	.150	.180	.180

TABLE 4. *Maximum intrusion of measured shoulder stresses into the parallel part of the specimen, represented by the length of the line XY, Fig. 5.*

1	2	3	4	5	6
		Intrusions at various widths of W.			
Curvature	A 1.0	B .8	C .65	D 575	E .525
1/2	.07	.05	.02	.01	.00
1	.045	.03	.015	.005	.00
1−1/2	.028	.02	.01	.00	.00
2	.02	.01	.00	.00	.00
2-Cat	.116	.147	.170	.180	.200

Although Table 3 shows that XZ is roughly independent of W, Table 4 and the dotted lines of Fig. 6 show that the length XY decreases for all curves HK shown in Fig. 4, with decreasing W except the catenary 2/1. The dotted line NYN Fig. 5 indicates the boundary of a region where the change in the value of $P-Q$ from the value of P in

TABLE 5. *Maximum tension in the specimen (at m, Fig. 5) when the average tension in the narrow part is 1000 lbs per square inch.*

1	2	3	4	5	6
		Maximum tension at various widths of W			
Curvature	A 1.0	B .8	C .65	D .575	E .525
1/2	1350	1210	1085	1028	1000
1	1120	1120	1085	1015	1000
1-1/2	1060	1000	1000	1000	1000
2	1000	1000	1000	1000	1000
2-Cat	1350	1350	1350	1350	1350
4-Cat	1060	1060	1060	1060	1060

the narrow part of the specimen is about 6%. Since $Q=0$ in the narrow part of the specimen generally this will mean that the value of Q at Y is 6% of the value of P at Z and there will be very little change in the value of P between the points Z and Y.

Table 5 has been prepared to show the relation between the curve HK, and the maximum tension in the member at the point m, Fig. 5. Rows 3, 4, and 5 show little or no increase in stress due to the shoulders,

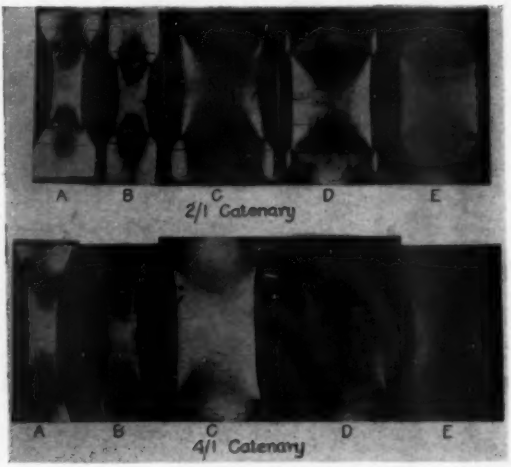

FIG. 7. *Photographs by the photo-elastic method of stresses in tensil test members with catenary curves in the shoulders.*

and rows, 4, 5, and 6 show no increase in stress with increase in width of shoulders. The catenary curves give less distortion of the stresses than any of the arcs of circles; (rows 1-4) therefore photograph of the catenary curves 2/1 and 4/1, A, B, C, D, and E are shown in Fig. 7. A comparison of A and E for each of the catenarys shows that stresses from the shoulder extend into the neck at an angle of about 45° independent of the curvature of HK and independent of the change in width HG.

STRESSES IN THE IZOD NOTCHED BAR

This investigation of the stresses developed in the different parts of the notched bar impact test number of the dimensions shown in Figs. 8 A and B, by the method of photo-elastic analysis has been carried on as a static problem with the bar subject to a load having the same direc-

tion and point of application (*a* Fig. 10) as the direction and point of application of the load for the dynamic tests for which the members were designed. In the dynamic tests the bar is supported at *b*, clamped at *c* as shown in Fig. 8 and broken by a blow at point *a* from a heavy hammer.

The distribution of stresses for a static load should give a very close approximation of the stresses resulting from the dynamic tests. This conclusion is supported by the generally accepted rule that impact tests for well annealed materials are independent of the velocity of the

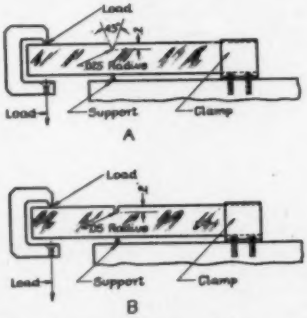

FIG. 8. *Load and support for notched bar test members.*

falling pendulum, a rule which can hold only when the stresses developed are independent of the velocity of the load applied at *a*.

The impact testing machines give as a result of tests made on them a measure of the work done in breaking the different test pieces. Nearly all of this work is used in deforming the piece by stresses beyond the elastic limit of the material being tested. This plastic deformation which determines the amount of work needed to break the specimen depends on the amount of material deformed and the extent of the deformation. The amount of material deformed must depend on the stresses surrounding points where failure will occur, which in turn must depend on the geometry of the notch. Therefore a map of these stresses has been made and a study of their dependence of the different elements of the notch has been carried out. The influence of three elements of the notch, the slope of the sides, the radius of curvature of the base and the ratio of the depth of the notch to the width of the bar has been investigated and the results are reported in the following paragraphs.

The study of the notched bar introduced several problems requiring special methods of study. Changes in the stresses at the base of the

notch were so concentrated in an exceedingly small area it was not possible to determine the nature of the stresses at these points by the ordinary studies. The limit of accuracy of the work was considered as the limit to which accurate determinations of the stresses at the base of the notch, the point where failure of the member starts, could be carried. The optical method of measuring the change in thickness, by counting the passage of interference fringes (see Fig. 2) gave values of $P+Q$ for different points very close to the base of the notch. The closest work was done with a magnifying glass which gave a magnification of about five. With a freshly prepared test piece during the first day it was used, measurements of change in thickness were made to within 1/400 of an inch of the edge of the notch.

The errors of the observations made close to the edge are necessarily high because of the great variation in the value of the quantities being measured (see Fig. 9). Measurements have been made, however, on 70 different specimens and confidence is placed in the accuracy of the general trend of the curves of Fig. 15 where *A* shows the relation between the depth of the notch and the resulting stresses at the base while *B* shows the relation between the radius of curvature and the stresses developed at the base of the notch.

The standard Izod Impact Test bar and the method of applying the load to the bar are shown in *A* and *B*, Fig. 8. Loads actually used have been reduced for purposes of comparison to a load giving a tension at the bottom of the notch as determined by photo-elastic observation, of 1000 lbs. per square inch. This figure for the load, 21.75 lbs., is identical for all of the calculations, and is the load upon which the results shown in the Figs. 11, 12, 13 and 14 are based. Later a more accurare measurement of the stresses at the bottom of the notch by the optical method illustrated in Fig. 2 proved that for the load used the stress should have been about 2400 pounds per square inch instead of 1000 pounds as observed at first. Equation 2 and the photographs of Fig. 9 show that the rate of change in stress at the base of the notch is about 100 per cent per .01 inch, which explains the discrepancy noted.

Fig. 9 *A* and *D* shows photographs of the isochromatics at the base of a notch in a bar clamped at one end and stressed by a torque about the other. *B* and *C* show respectively the 80° and 30° isoclinic lines for the notch under the same conditions of stress. *E* and *F* show photographs of the isochromatic lines for the standard notched bar under the conditions of loading just described. Figs. 10, 11, 12 and 13 follow

a uniform plan and show for A maps of test members A respectively on a small scale. B is omitted except in Fig. 10 because it is nearly identical with A. D and C give maps of the respective notches on a larger scale. The lettering is identical for all figures.

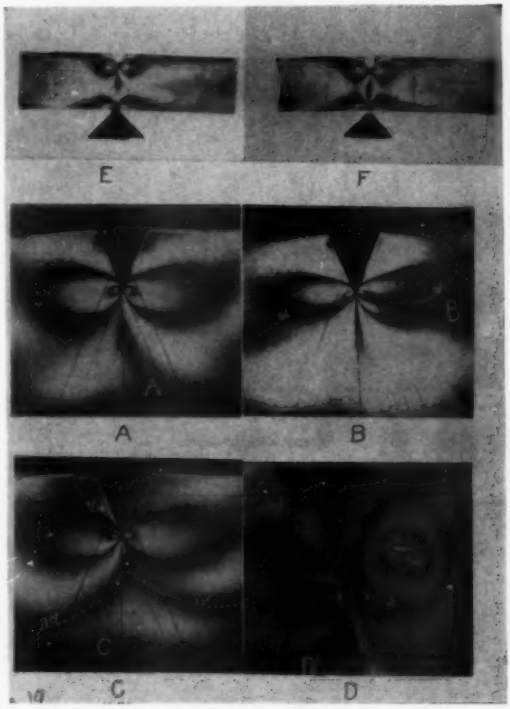

FIG. 9. *Photographs of stresses in notched bars. A, D, E, and F show isochromatic lines. B and C show isoclinic lines.*

Fig. 10 gives maps of the isochromatics or lines of equal value for $P-Q$. Small values of $P-Q$ in the region of the shoulders of the notch (*ee*) indicate that the slope of the sides of the notch are not an important element of the stress problem. This conclusion is verified by by the fact that in no important point was there a measurable difference of the stresses for specimens A and B.

Fig. 11 which gives maps of the isoclinics or lines of equal slope for the P and Q stresses shows at once several interesting elements of the

stress problem. At the point, (f), P and Q stresses have no definite direction. This condition is possible only for points where $P=Q$. The neutral point (f) lies on the central line of the specimen, that is 1/2 the

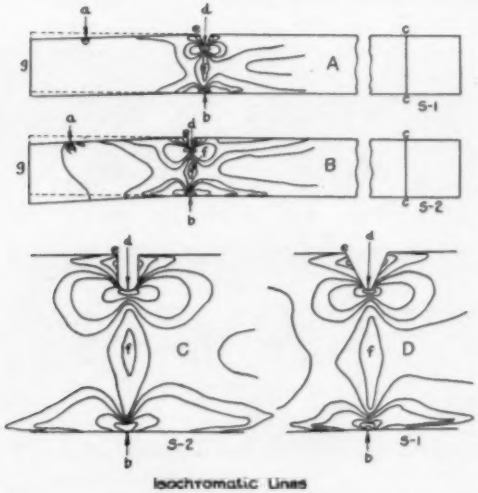

FIG. 10. *Map of $P-Q$ values for notched bar test specimen.*

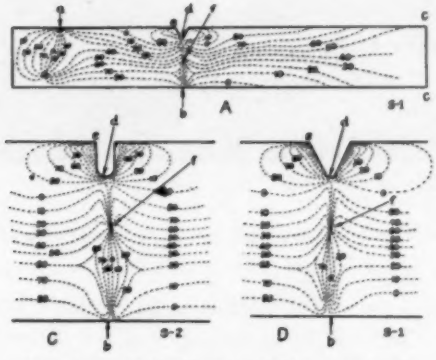

FIG. 11. *Isoclinic lines for notched bar specimens.*

width above the lower edge. This is the line of zero stress for a beam bent by a torque. Therefore the conclusion was drawn that at the point (f) all stresses due to the compression at the point (b) are balanced by stresses due to tensions about the point (d) and at the point (f) P and

Q are both zero. This conclusion was supported by micrometer measurements of the thickness of the specimen at the point (f). There was no measurable change in thickness with the application of the load.

The value of P and Q at the point (f) is important because this point

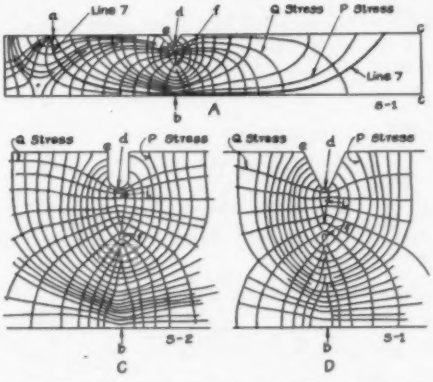

FIG. 12. *P and Q stress lines for notched bar test specimens.*

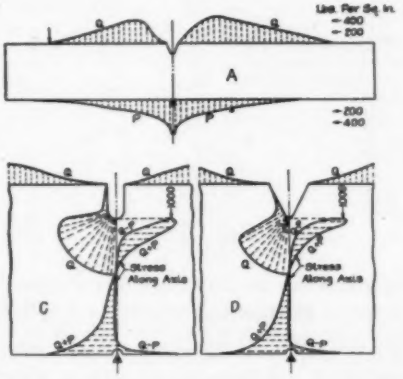

FIG. 13. *Tangential stresses for notched bar specimens.*

was used as a starting point for a number of integration. Satisfactory integration can not be carried from high to low values of $P-Q$, because the errors are carried along and increase in importance as $P-Q$ decreases.

Fig. 12 gives maps of the directions of the P and Q stresses for the specimens. Fig. 13 gives curves showing the tangential stresses at different parts of the boundary. These values are taken directly from

the isochromatic maps of Fig. 10. Since the normal stresses are always zero at the boundary where there are no external forces the value of the isochromatic $Q-P$ gives a direct measure of the value of the tangential force. The values for P and Q along bd were obtained by integration.

The maps of Fig. 12 show that near the base of the notch the Q stresses are parallel to the base of the notch and hence have a radius of

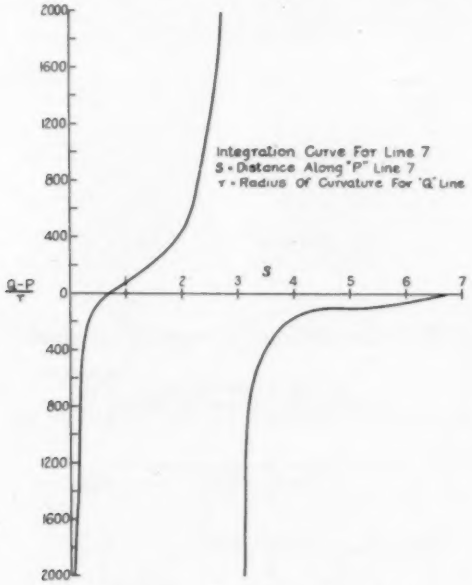

FIG. 14.

curvature equal to the radius of curvature of the base plus the distance from the edge; therefore at the base of a sharp angle where the radius of curvature is zero according to equation (6), the rate of increase in Q must be infinite unless $P-Q$ is equal to zero at the base of a sharp angled notch. A very careful investigation of this question by the photo-elastic method of evaluating $P-Q$ along the edge of the notch indicated quite clearly that the tension parallel to the edge of the notch is a maximum a slight distance above the base of the notch. This distance is small, being less than a hundredth of an inch for standard test member and no measurements were possible.

In general the distribution of the load on a bent beam is of influence only in the immediate neighborhood where it is applied and we may

conclude that the stresses near the notch are due to the curvature of the bar only and that stresses due to the surface traction from *a* and *b* are a negligible factor. The problem then is reduced to the question of the stresses surrounding a notch in a bar bent by a torque. Photographs *A* to *D* Fig. 9 show the appearance of the field of stresses due to a sharp angled notch. *D* is a 3/1 enlargement of A. This simplified

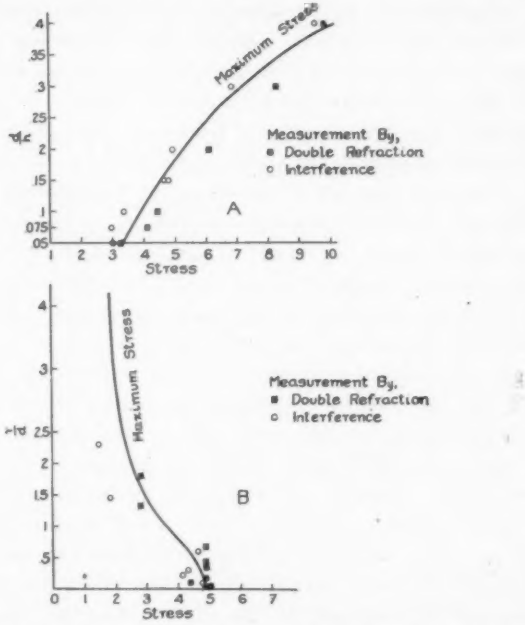

FIG. 15. *Relation between stress at the surface of an unnotched beam bent by a torque about each end and the maximum stress at the base of a notch in the same beam, A, with varying depth of the notch, B with varying curvature at the base of the notch.*

problem has been studied in detail. The results of the investigation are shown in the two curves of Fig. 15 where the abscissa in each case is the stress at the base of the notch when the bar is loaded with a torque sufficient to give unit stress at the surface of an untouched bar.

For *A* the ratio of the width of the beam (h) to the depth of the sharp notch (d) is taken as ordinate. The smooth curve for this Figure is drawn by the equation:

$$S=3+4\{[h/(h-d)]^3-1\}=4[h/(h-d)]^3-1 \qquad (8)$$

which was obtained empirically. In this equation 3, the value of S for a circular hole at the edge of an indefinite plate[8] is found to be the value of S for d equal to zero.

For B the ratio of the radius of curvature at the base of the notch (r) to the depth of the notch (d) is taken as ordinate. Thus the curve shows the relation between the radius of curvature at the base of the notch and the increase in stress due to the notch. The curve shows that the stress is independent of the curvature if the radius is small as compared with the depth of the notch. This one point was investigated very carefully and for values of r/d from zero to .5 no change could be detected.

The following conclusions have been reached as a result of this investigation. The purpose of the Izod test is the obtaining of a figure which is proportional to the ability of the tested metal to resist a shock. The test gives a measure of the energy of deformation during rupture and this will depend on the stress developed at the base of the notch. The maximum stress developed at the base of the notch in a notched bar test member of the ordinary design is independent of the radius of curvature of the base, if the radius is small. This conclusion is supported by the work of Thenard[9] who by a series of tests proved that, although the Izod test number for steel specimens may vary by as much as 100% for very slight changes in the elastic properties of the steel and different specimens of a very uniform steel may give a test number which varies by 100% with carelessly prepared notches, a uniform steel will give a uniform test which will be independent of the radius of curvature of the notch if the surface of the notch is free from surface hardening. The curvature of the notch, however, has an important influence on the surface hardening and the effect can change the Izod test number (Glazebrook[10]). In the notched bar both the volume deformed and the velocity of the deformation are dependent on the elastic properties of the material. One obvious method of obtaining more consistent time and volume factors for the deformation has been suggested by Coker, who advised the adoption of a bar notched on both sides and broken by an impact tension. Obviously, with such a test member the time or velocity of the deformation would be under much better control. Moreover, since the stress would be more uniform across the breaking section, the volume deformed and the velocity of deformation at one point would be nearly independent of what happened

[8] Prescott's "Applied Elasticity," p. 361; 1924.
[9] Iron and Steel Inst. Journ., No. 96, p. 61; 1917.
[10] Dictionary of Applied Physics. p. 205; 1922.

at any other point. For these reasons it would seem advisable to give the double notched bar a practical test.

Steel when subjected to repeated loads beyond the elastic limit becomes brittle. The engineer is interested directly in this "induced" brittleness. The Izod test is a roundabout way of obtaining a figure which is supposed to be inversely proportional to the brittleness of the metal. The following suggestion is offered as a means of obtaining a more direct test of the property of the metal which causes failure under impact.

It is suggested that a double notched bar be subjected to an impact load as near the breaking load as can practically be applied without causing failure and then be immediately subjected to a second breaking load. Specifications for a material would then state that the impact specimen must not fail under a given impact and must show a specified energy of failure immediately following the impact. Such tests could, of course, be compared at any time with the energy of failure for a breaking load at the first impact and these comparative figures might give valuable information concerning the material being tested. Thus with the addition of one unrecorded operation to the test two new items might be added to the specifications for the material, which could then state the energy of rupture under impact, the impact to be withstood without failure of the test piece, the energy of rupture after an initial impact and finally the ratio of the initial strength to the strength after overloading the impact.

SHIP PROPELLER SHAFT STRUTS[11]

The designing of propeller shaft struts calls for a knowledge of the stresses in the different parts of the struts under conditions of loading which lead to failure of a strut. Failure will generaly start at a point of maximum stress when the stress at this point exceeds the ultimate strength of the material, therefore both the location and the magnitude of the maximum stress with reference to some given load on the propeller shaft is of first importance. Attention has been confined throughout this study to the relation between the maximum stresses in the strut for a given load and eccentricity of the strut with reference to the center of the propeller shaft. This eccentricity of the strut is represented by the length of the line *oe*, Fig. 16. All other factors of the stress problem were kept constant.

Fig. 16 shows photographs of the different strut members tested.

[11] A brief account of the problem has appeared in the Pro. Am. Soc. Nav. Arct., *34*, p. 119; 1926.

These pyralin struts are cut to represent sections of actual propeller shaft struts taken perpendicular to the shaft through the thickest part of the strut. The lettering and description of I, Fig. 16 is used in speaking of the different struts. The angle *agb* is 40° and the angle *agc* 20° for each member. A load was applied at the point *o* in the direction *of* perpendicular to the line *oc*. The thickness of the strut, *hi* is 5/19 of the radius of the section of the bearing housing *oc*. The line *eo*, for I is 3 times the thickness of the strut, for II, is 1.5 times the thickness of the strut, for III is 0, and for IV it is .5 times the thickness of the

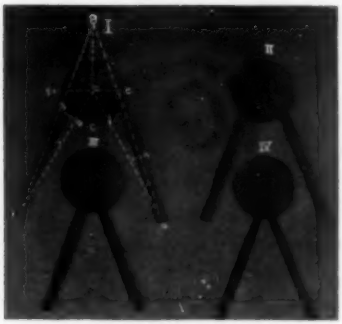

FIG. 16.

strut. The housing of the propeller bearing is so much stiffer in its construction than the supporting struts that its cross section is not appreciably deformed by stresses in the struts, consequently, this section was made solid as shown in the photographs.

The drawings and photographs of Fig. 17, 18, and 19 show maps of the stresses in struts with eccentricities as shown respectively in photographs I, II and III of Fig. 16. Only that part of strut near the housing of the bearing is shown because stresses which might lead to failure are found only there.

The value of $P-Q$ at the points x and y of B Fig. 17 and 18, is approximately zero. The value of Q from either of these points to the inner side of the strut is approximately zero, therefore the isochromatics of A give a close approximation of the value of the P stress for this region The value of P from either of these points to the outer side of the strut is approximately zero and the isochromatics of the outer part of the strut give approximately the value of the Q stress for this part of the strut. It is then obvious that the points of maximum stress are to be

found at the boundaries of the struts where maximum values of the isochromatics are located.

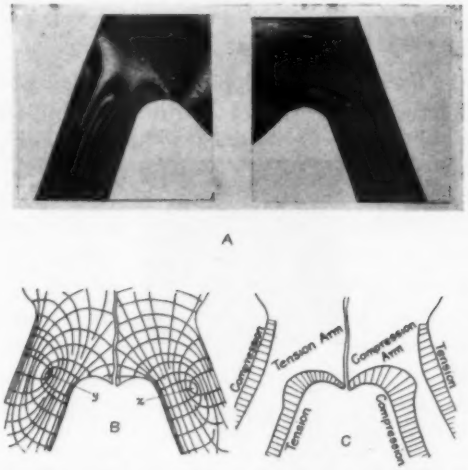

FIG 17. *A, isochromatic lines; B, P and Q stress lines; C, tangential stresses for propeller strut I.*

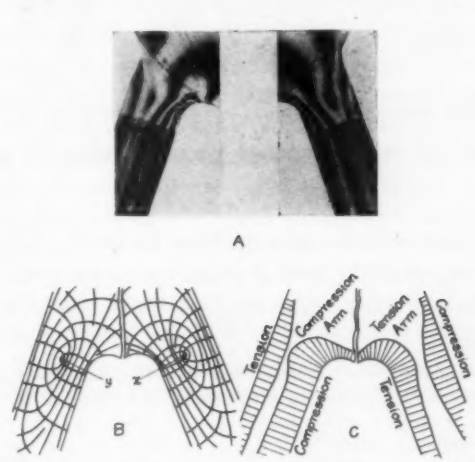

FIG. 18. *A, isochromatic lines; B, P and Q stress lines; C, tangential stresses, stresses for propeller strut II.*

Each strut studied apparently acts as an eccentrically loaded column supported at *a* and *b* (Fig. 16) and loaded at *o* the center of the shaft.

The horizontal load applied at O was resolved into two components directed toward the points of support along the lines *oa* and *ob*. Each strut was then subject to a compressional or tensional load given by the equation:

$$L' = L/2 \sin \phi \tag{9}$$

where L was the horizontal load applied at o and ϕ was the angle *aoc*. The total load across any section of a strut was found to be the direct

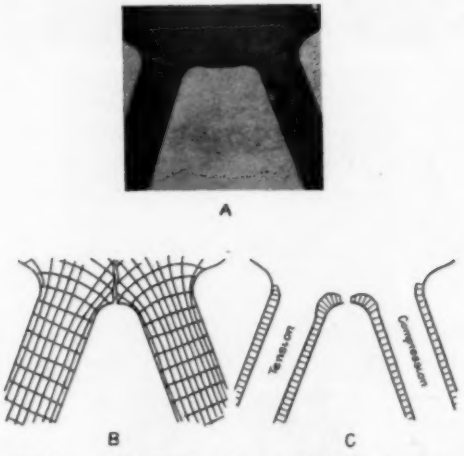

FIG. 19. *A, isochromatic lines; B, P and Q stress lines; C, tangential stresses for propeller strut III.*

direct compression or tension load plus a torque (T) given by the equation:

$$T = L' \cdot d \tag{10}$$

where d is the perpendicular distance from the line of action of the load *oa* to the mid-section of the strut *ga* at the considered point. The torque was of course a maximum at the point where the strut joined the housing. Table 6 gives values of direct load and maximum torque for the

TABLE 6. *Maximum torque on struts under 2 lbs load at O.*

1 Strut	2 Eccentricity *oe*	3 Load on strut L	4 ϕ	5 Distance *mm*	6 Torque calculated	7 Torque measured
I	1.5	2.015	29.5	1.03	2.075	1.927
II	.75	2.34	25.30	.58	1.357	1.204
III	.000	2.92	20.00	.00	.000	.000
IV	− .25	3.24	18.00	.27	−.875	− .81

struts studied when a load of 2 lbs. was applied at O perpendicular to oc. Column 1 gives the strut studied, Column 2 gives the eccentricity of the strut or length of the line oe, Column 3 gives the direct load or force from o to a, Column 4 gives the angle ϕ, column 5 gives the torque distance mm, Fig. 16, Column 6 gives torque obtained by 10 and the figures of column 7 were obtained by applying a torque about 0 (equal parallel forces oppositely directed) sufficient to reduce the stresses in the struts to compression and tension only. This condition was easily determined photo-electrically since then and only then was the stress uniform across any section of the strut.

These studies show that propeller shaft struts should be designed like Strut III so the center lines of the struts meet at the center of the propeller shaft. In this case the distance mm is zero and the torque across any section of the strut is zero. The only load on either strut is then the direct compression or tension load which is uniform across the entire section of the strut. Such a design will give the lowest maximum for the stresses in the strut, as shown by the photograph and drawings of Fig. 19.

GUN TURRET ROLLER PATH RING

The battleship gun turret rests and turns upon cone shaped rollers which travel in a circular path cut in an immense casting known as the "roller path ring." When a gun is fired the recoil momentum of the gun must be transmitted from the turret to the ship through this ring which is loaded front and back by forces opposite to the direction in which the gun is pointed. The ring is irregular in cross section and the loading and support are of course very complex but for the purpose of this study the entire problem has been simplified to a study of stresses in a flat ring loaded and supported as shown in Fig. 20.

Three specific questions are answered in the following study of stresses in a flat ring. *First*: What is the strength and stiffness of flat rings of uniform section loaded and supported as shown in Fig. 20 A and B? The answer to this question is in the tangential stress curves of Figs. 23 and 24. The load applied in pounds to produce these stresses was in each case equal to 400 times the cross section of the ring in square inches. *Second*: What is the bending moment at a given cross section of a ring loaded as shown in Fig. 20, A and B? For the loading conditions given above this question is answered by the torque curves in Figs. 23 and 24. A geometrical solution of the problem is presented in Fig. 25. *Third*: How is the bending moment affected by substitution

of loading forces spread through moderate ranges of arc instead of concentrated at the points *bb*. This question is answered by a comparison of the photographs of Fig. 20.

Rings 4″ in diameter cut from pyralin 1/4″ thick were loaded and supported as shown in Fig. 20. The loads *b b′* were spaced 180° apart and 90° from the points of support *a a′*. The loading forces were parallel to the supporting forces. One point of support was pivoted and free

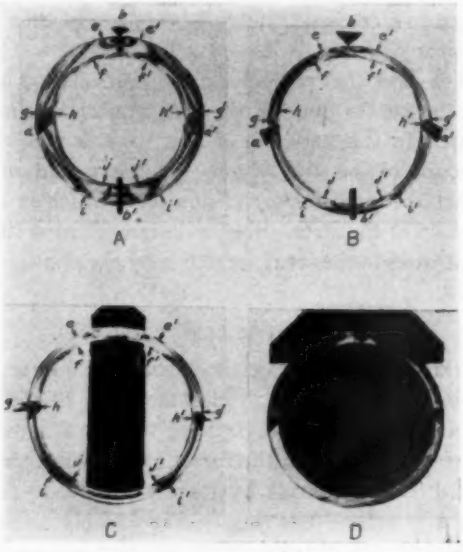

FIG. 20. *Isochromatic lines for rings supported at the points a a′ and loaded by forces normal to the line a a′.*

to move at right angles to the load and allow the ring to deform. The loads *b* and *b′* were equal in rings *A* and *B*, but with rings *C* and *D* a solid core transmitted the load from the top to the bottom of the ring keeping the distance *b b′* constant irrespective of the relative values of the loads. The loading for rings *C* and *D* is considered to approximate more closely the conditions of loading of the roller path ring when the turret guns are fired than the loading of *A* and *B*. On the other hand the loading of rings *A* and *B* furnishes a simpler mathematical problem and gives, therefore, simpler conditions for a study of the general problem of stresses in a loaded ring. This paper deals principally with this type of loading. Different steps in the study were performed with

different loads on the ring which of course is deformed slightly, becoming heart shaped. The whole problem has been simplified by presenting ing the results on the undeformed ring. This is of course an approximation but it is a very close one.

The photographs of Fig. 20 show lines of constant color or isochromatics for the rings studied. The points e, f, g, h, i, j, and $e', f', g',$

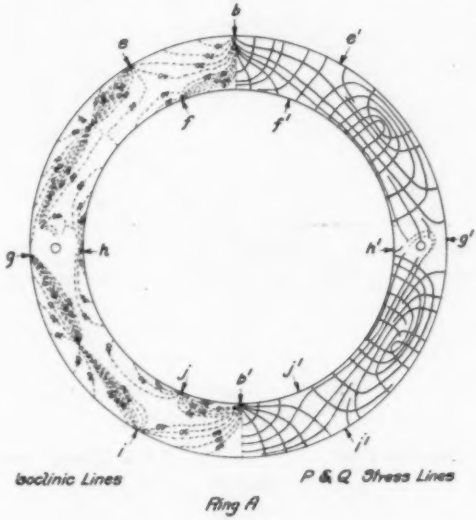

FIG. 21.

h', i', j' on the photographs mark points of zero value for the tangential stresses. These "principal points" are of first importance because they outline the stress map of the entire specimen.

Rings B, C, and D (Fig. 20) were each given the same load (50 lbs. total). The pictures show at once the great effect of the concentration of the load. The photographs show that the stress diagram is symmetrical about the vertical diameter therefore in the following figures (21 to 25 inclusive) only one half of the ring is shown for each map.

Figs. 21 and 22 show isoclinics or lines of constant slope for the stresses on the left and stress lines constructed from this map on the right. In these figures the principal points are seen to be places where the stress becomes zero and the direction is indeterminate. This is shown by the convergence of isoclinic lines and by the reversal of the relative positions of the P and Q lines.

The left side of Figs. 23 and 24 show the tangential stresses, plotted so the lengths of the radial shading lines are everywhere proportional to the magnitude of the tangential stresses at the points where they touch the circumference of the ring. Lines drawn *away from* the ring represent *tension* and lines drawn *into* the ring represent compression. Here again the principal points are of special interest. If we call the set of stress

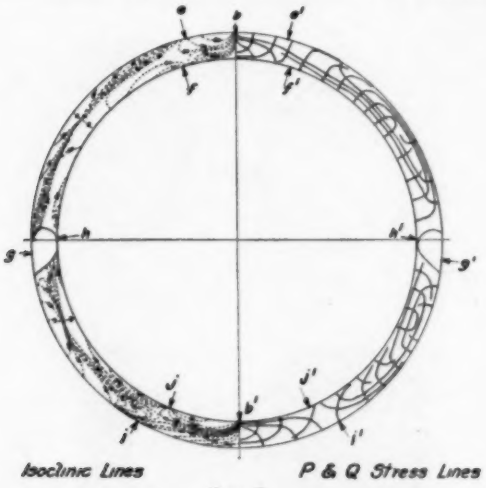

FIG. 22.

lines shown in Figs. 21 and 22 radiating from the points b' "P stresses" we see at once that the tangential stress not only becomes zero at the principal points but also that its direction is indeterminate. Thus the tangential stress is a "P stress" from b to e, from f to g it is a "Q stress," from g to i it is again a "P stress," and the last reversal makes it a "Q stress" from i to b'. Similar changes can be followed along the inner edge of the ring.

Figs. 23 and 24 show torque (pounds per sq. in. times inches) across different sections of the rings plotted as lengths of the radial lines measured from the middle of the ring.

Values of torque for the solid curves are measured and calculated by the use of the equation for torque in a bent beam.

$$T = 1/3Fd^2 = 1/3Std^2 = 1/12Sd^2 \qquad (11)$$

where S is the tangential stress, t is the thickness of the ring (1/4") and

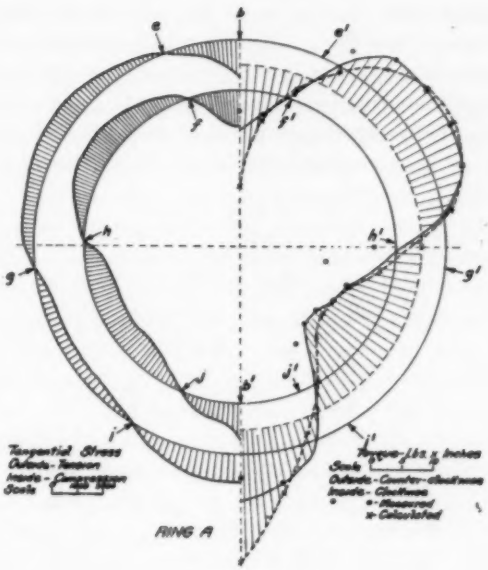
Tangential Stress
Outside - Tension
Inside - Compression
Scale
Torque - Lbs. x Inches
Scale
Outside - Counter-clockwise
Inside - Clockwise
o - Measured
x - Calculated
RING A

FIG. 23.

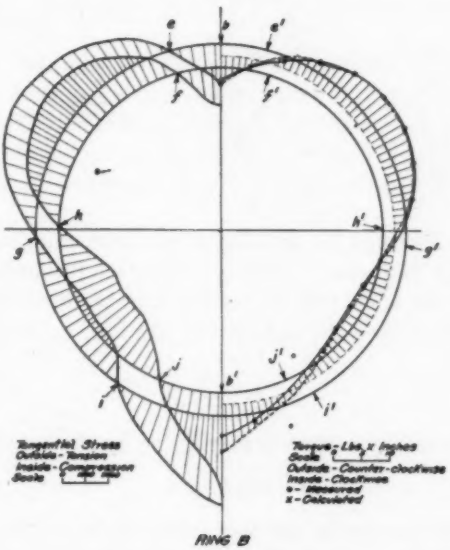
Tangential Stress
Outside - Tension
Inside - Compression
Scale
Torque - Lbs. x Inches
Scale
Outside - Counter-clockwise
Inside - Clockwise
o - Measured
x - Calculated
RING B

FIG. 24.

d is the perpendicular distance from the edge of the ring to the line of minimum value for $P-Q$. These calculations are based on the assumption that the change in stress across the section is uniform. This is obviously not true for certain sections i.e., at a and at b.

Fig. 25 shows the method used to calculate the torque, plotted in the broken lines curves, across any section of the rings. The direction of

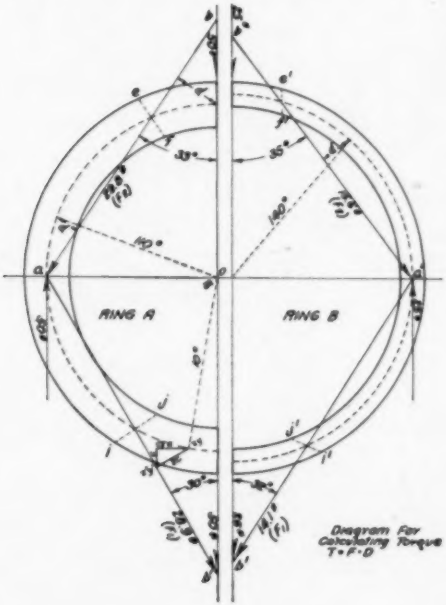

FIG. 25.

the load ba is obtained by drawing a line from the point of support (a or a') through mid point of the line connecting two opposite principal points (ef). If the angle this line makes with the direction of the load L applied at b is ϕ, then the equation for the load on a quadrant of the ring is:

$$F = L/2 \cos \phi \tag{12}$$

The torque across any section is then given by the equation:

$$T = Ld/2 \cos \phi \tag{13}$$

where d is the perpendicular distance from the line of the load F to the middle line of the ring. Again the principal points are of special interest,

since at cross sections of the ring between two nearly opposite principal points, the direction of rotation of the torque is reversed.

Photographs *B*, *C*, and *D* of Fig. 20 show the same ring with equal loads (50 pounds total) which were distributed over different arcs. They show at once that the regions of greatest stress were found near the points of contact between the ring and the edge of the loading frame. This results from the fact that the loading frame is much stiffer than the ring and therefore constrains the section in contact with it to remain an arc of a circle. *B* with a concentrated load showed a maximum stress due to torque of 2500 lbs. *C* with the load spread over an arc of 20° showed a maximum stress of 1800 lbs. *D* with the load spread over 100° showed a maximum load of 800 lbs.

A flat ring under load is subject to different types of stress which may cause failure. First, there are local stresses due to surface contacts. When the load is distributed over a wide angle and the ring is not allowed to deform these contact stresses are of first importance as is shown by the photographs of Fig. 20, *C* and *D*. When the ring is allowed to deform, stresses resulting from the deformation are of first importance as is shown by the photographs *A* and *B*. If the load is distributed over a small arc by a frame which is stiffer than the ring, maximum stresses will be found at the edges of the distributing frame, as is shown by photograph *C*, Fig. 20.

The geometrical solution of equation 13 shown in Fig. 25 is applicable to any ring loaded and supported as shown in Fig. 20 *A* and *B*. This solution will also give results which are approximately correct at points of maximum torque for rings which are nonsymmetrically loaded and supported, when the torque about the point of support is small.

NAVAL RESEARCH LABORATORY,
WASHINGTON, D. C.

A POTENTIOMETER ARRANGEMENT FOR THE MEASUREMENT OF EMF OVER A WIDE RANGE

By C. D. Miller

It is often desirable to measure emf without drawing current from the source of the emf, and it sometimes happens that a potentiometer of suitable range is not available. For example, the Leeds & Northrup Students Potentiometer alone is not suited to the measurement of such emf as is obtained with a base metal thermocouple at furnace temperatures of the order of 50 millivolts, this being too low for the 1.6 volt range and too high for the 16 millivolt range. Again, it may be desirable to avoid the use of a standard cell, or a voltmeter may be available which would be entirely adequate if it were of suitable range, or if it drew no current. This arrangement is adapted to use under such conditions, affording the advantage of a widely flexible range, and when used in connection with a voltmeter, something of the advantages both of a potentiometer with standard cell, and of an indicating instrument. It may be used with either a potentiometer with standard cell, or with a voltmeter, to reduce the range as desired, affording an order of accuracy that is substantially the same as that of the potentiometer or voltmeter when used over its own range, alone. It is most convenient when used with a voltmeter, and the order of accuracy is entirely sufficient for most purposes other than the calibration of electrical instruments, even with a voltmeter of only moderate accuracy. In the measurement of temperatures from 0 to 100 by means of a thermocouple, using a very inexpensive voltmeter and a portable galvanometer in the arrangement, I have obtained as great accuracy as is obtained with an ordinary mercurial thermometer, being able to estimate easily to one-tenth degree, and the arrangement has proved to be simple in operation, and quick and easy in adjustment and reading.

The arrangement is shown in its essentials in Fig. 1. The galvanometer G is in series with the source of the emf to be measured, and this emf is balanced by the potential difference existing between the connections to the resistance A. The resistances A and B are calibrated and adjusted to give a simple, convenient value to the ratio $A/(A+B)$, so that the value of e can be read at once on the voltmeter V when the circuit is properly balanced. The balancing is accomplished by adjustment of the

resistances R and P, so that the galvanometer indicates no current. An adjustment of the resistances A and B permits the measurement of any range of emf up to the full scale reading of the voltmeter. If the arrangement is used to provide a low range for a potentiometer, the potentiometer simply replaces the voltmeter for the measurement of the potential difference V. The galvanometer must of course be of suitable sensitivity, and the accuracy of the resistances A and B must be suited to the accuracy to be attained in the measurement.

It will be seen that the battery emf E, battery resistance, values and adjustment of R and P, the current taken by the voltmeter and that

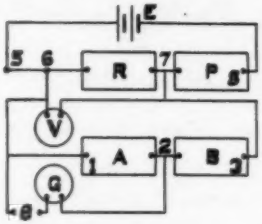

FIG. 1. *General arrangement for the measurement of emf.*

passing through A and B are matters of no concern so long as they permit satisfactory adjustment of V, the potential difference across A and B, indicated by the voltmeter, so that no current passes through the galvanometer.

In the selection of the resistances A and B, two methods for the adjustment of the ratio $A/(A+B)$ are to be considered. By one method, the sum $A+B$ is kept constant; by the other, A is kept constant. Each method has its advantages. If the sum $A+B$ is kept constant, there is the advantage that the adjustment of R and P is the same for all values of the ratio $A/(A+B)$. In this case, however, the resistance of the galvanometer is not the same for different values of $A/(A+B)$, being small for small values of the ratio, and large for large values. This may be an advantage, in that small values of the ratio are required for the measurement of small values of emf, requiring the galvanometer to respond to very small changes in e, while for larger values of e the resistance of the galvanometer circuit is greater, which automatically prevents the galvanometer from responding too much to a small change in e in this case. If A is kept constant, adjustment of R and P is affected by adjustment of the ratio $A/(A+B)$, but this may not be great enough to make trouble. The resistance of the galvanometer circuit is approxi-

mately the same in this case for all values of $A/(A+B)$, so that the galvanometer is almost uniformly sensitive to a change in e, no matter whether the value of e be great or small, and further, the galvanometer will remain suitably damped if the resistance of its circuit is once adjusted. That is, considering the resistance of the source of emf to remain constant. In this connection, it is to be noted that for the measurement of small values of emf, B is so much greater than A that the resistance of the galvanometer circuit is substantially the sum of A, the resistance of the source of emf, and the resistance of the galvano-

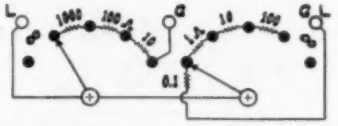

FIG. 2. *Series and shunt resistance box for the control of the galvanometer.*

meter itself. Further, it is to be noted that a suitably adjustable resistance is required to protect the galvanometer while V is being adjusted. Fig. 2 illustrates a combination of series and shunt resistances that I have found convenient. This permits the adjustment of V through successive stages of increasing accuracy, without danger to the galvanometer and without the inconvenience of excessive deflections, the complete adjustment of V being accomplished conveniently and quickly in this way.

If the sum $A+B$ is to be kept constant, two ordinary resistance boxes will serve, or a single plug box with two travelling plugs can be used. Fig. 3 illustrates a special potentiometer or ratio box that I have found convenient. The numerals 1, 2, 3, Figs. 1, 3, show how the box is connected. This box gives the following values of the ratio $A/(A+B)$:.001, .002, .005, .01, .02, .05, 0.1, 0.2, 0.5, 1.0. These are the values of the ratio e/V, so that with the decimal point properly placed, e is read directly on the voltmeter scale, or by multiplying or dividing the voltmeter reading by 2. This series of values is also of advantage in that the voltmeter scale need not be used below four-tenths of its full value, which eliminates the inaccuracy attendant upon the use of lower parts of the scale.

If A is to be kept constant, a single resistance for A and an adjustable box for B are all that are required. A special dial box illustrated in Fig. 4 will also serve, giving the same values of e/V as noted in connection with Fig. 3. The resistances shown in Fig. 4 are greater than those shown in Fig. 3, in order that the value of $A+B$ shall not be so small as to cause

inconvenience in the amount of current taken when B is given its smaller values. This is important since the amount of current affects the adjustment of R and P.

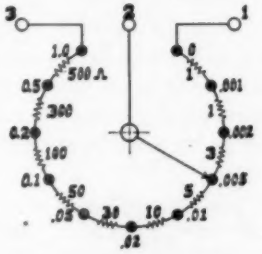

FIG. 3. *Ratio box constituting the resistances A and B, arranged to keep A+B constant.*

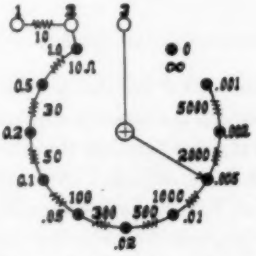

FIG. 4. *Ratio box constituting the resistances A and B, arranged to keep A constant.*

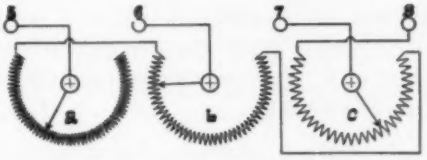

FIG. 5. *Arrangement of rheostats constituting the resistances R and P.*

Fig. 5 illustrates a convenient arrangement of rheostats to provide the resistances R and P. I have found radio dial rheostats to be convenient here. Rheostat a, like the resistances A and B, is not ordinarily involved in an adjustment of V and measurement of e. With A and B adjusted to give a suitable ratio e/V, a is adjusted so that the voltmeter needle can be made to go a little beyond the full scale point by adjustment of b and c, c serving simply as a fine adjustment, being of 1/10 or 1/20 the resistance of b. Rheostats of 400 and 20 ohms, provided

with the potentiometer connection as illustrated, have served me satisfactorily for b and c. The connections are arranged so that V is increased by clockwise rotation of a, b, or c.

To permit ready and accurate adjustment of V, it is necessary to have the resistances of a, b, and c suitably proportioned to that of the voltmeter in combination with A and B. The resistance of this combination remains fixed in the course of an ordinary adjustment of V, and it is convenient for mathematical purposes to consider the combination to be replaced by a single resistance J in parallel with R. It is also con-

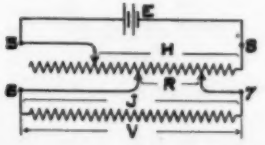

FIG. 6. *Elements of the arrangement affecting the adjustment of the pd given by the voltmeter, V.*

venient to denote the sum $R+P$ by the symbol H. The mathematical essentials of the arrangement as regards adjustment of V are shown in Fig. 6. V is the potential drop through the fixed resistance J, E is the emf of the battery, H is to be adjusted to a suitable fixed value, while the actual adjustment of V is to be effected by adjustment of R. V is to be regarded as a function of the constants E, J, H, and of the variable R. A constant ratio V/R represents the ideal relationship, but on account of the resistance J in parallel with R this can be only approximated. However, by a suitable selection of resistances this approximation can be readily made close enough to permit easy and accurate adjustment of V. This can be seen from the curves of Fig. 7, computed from the relationship

$$V/E=1/(H/R-R/J+H/J) \tag{1}$$

These curves indicate that the smaller H/J, the better, while at the same time little is gained by reducing the value of H/J below unity. Other considerations may however make it very desirable to use greater values of H/J, and the straightness of the curves in a certain region shows the possibility of doing this with satisfactory results. There is in fact a point of inflection, the locus of which is shown ranging from the point $R/H=1/3$, $V/E=1/3$ for $H/J=0$ to the point 0, 0 for $H/J=\infty$. This locus is given by the equation

$$V/E=(R/H)^3/(1-2R/H)^2 \tag{2}$$

In case the greatest value of V is to be small in comparison to E, it may be desirable to use a very large value of H/J. The nature of the curves in this lower region is shown by Fig. 8, in which $(H/J)V/E$ is plotted in place of V/E as a function of R/H, and the locus of the point of inflection is shown correspondingly. In the consideration of these curves, it is important to note that with the series of values of the ratio e/V given by the ratio boxes of Figs. 3 and 4, and with the ready

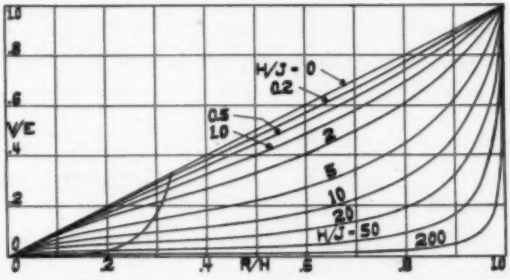

FIG. 7. *Curves giving V/E as a function of R/H, for values of H/J ranging from zero upward.*

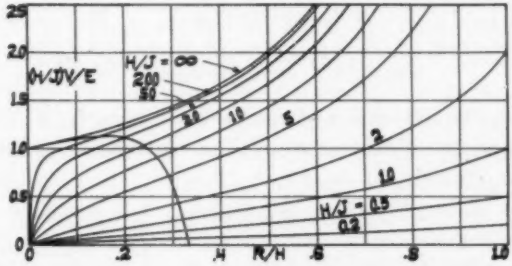

FIG. 8. *Curves giving $(H/J)V/E$ from zero to 2.5 as a function of R/H, for values of H/J ranging from infinity downward.*

change from one value of the ratio to another, the value of V need never be adjusted to anything less than four-tenths of the full scale of the voltmeter. For example if the value of $(H/J)V/E$ is 2.5 to get the full scale reading of the voltmeter, then no value of $(H/J)V/E$ less than unity need be used. In view of this and of the fine adjustment provided for R, it will be seen by Fig. 8 that there is no limit to the value of H/J, so long as a great enough value of V is obtained when $R/H = 0.6$. In this connection it is important to note some approximate expressions for the relationship between V and R, in special cases. For very small values of H/J, R/J is also small and $V/E = R/H$, the ideal relationship.

For very large values of H/J and values of R/H that are not close to zero, R/J is large and approximately $V/E=J/(H-R+J)$, giving

$$V/E=1/(H/J-R/J+1) \tag{3}$$

If further R/H is not close to unity, $H/J-R/J$ is large and (3) reduces to $V/E=1/(H/J-R/J)$, which gives

$$(H/J)V/E=1/(1-R/H) \tag{4}$$

This gives approximately the values of V for large values of H/J, over the useful range of R/H mentioned in connection with Fig. 8.

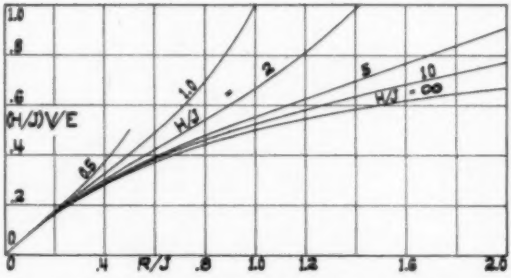

FIG 9. *Curves giving $(H/J)V/E$ as a function of R/J, for values of R/J from zero to 2.0, and for values of H/J ranging from infinity downward.*

Representing the full scale reading of the voltmeter by V_1, and the value of R necessary to obtain it by R_1, and letting $R_1/H=0.6$, there is obtained

$$V_1/E=2.5J/H \tag{5}$$

which gives approximately the value of H required for given values of V_1, E and J, to utilize the favorable region for large values of H/J that has been noted in connection with Fig. 8. The pronounced bend that developes in the curves, approaching the point 0, 1.0, puts a lower limit to the values of V that can be obtained with convenience and accuracy, which as noted is substantially at or below four-tenths of the value of V obtained when $R/H=0.6$, and may therefore not result in any inconvenience in measuring small values of e, since this part of the scale need not be used, and should not be used for accurate work. By having the entire adjustment limited to a region below the bend, however, the entire scale of the voltmeter becomes available to use, though the more of the scale is used, the more noticeable and troublesome becomes the deviation from the linear of the V, R relationship.

To bring out the character of the V, R relationship below the bend, $(H/J)V/E$ has been plotted against R/J, Fig. 9. It will be seen from these curves that any value of H/J will permit good adjustment of V over the range obtained with values of R/J from zero to unity, so that if H is such that $R/J=1$ will make $V=V_1$, then convenient adjustment can be had over the entire range of the voltmeter. For $H/J>10$ and $R/J\leqq 1$, the equation

$$V/E=1/(H/R+H/J) \tag{6}$$

gives approximately the relationship between V and R. Letting $R_1/J=1$ there is obtained

$$V_1/E=0.5J/H \tag{7}$$

which gives approximately the value of H required for given values of V_1, E and J, to utilize this lower range of values of R.

This arrangement I may say is not altogether new, but it does not appear to have been described previously in the literature, and I worked it out independently as described here, to meet my own needs. A similar but rather more elaborate arrangement, for measurements of high precision, has been reported on by A. W. Gray,[1] and I am indebted to Dr. Gray for describing his arrangement to me recently in private correspondence. The arrangement itself I have apparently worked out in more detail than he has done, as I believe to be justified by its great adaptability. I am also indebted to Dr. H. B. Brooks of the Bureau of Standards for pointing out to me the advantages of changing B only, as shown in Fig. 4, instead of changing both A and B as shown in Fig. 3, and for other very helpful suggestions and criticisms in connection with this paper.

WASHINGTON COLLEGE,
CHESTERTOWN, MD.

[1] P. R., *14*, p. 541.

Trace of mercury easily detected.—As small a proportion as one part of mercury in 20 000 000 parts of the atmosphere can be measured accurately by a device which has been developed in the research laboratory of the General Electric Company; one in 8 000 000 parts can be determined quickly.

Mercury poison is accumulative; it seems to make little if any difference whether the amount of vapor is inhaled as relatively large amounts in a short period of time, or as slight amounts over a period of months. Because of the increased industrial use of mercury in heating operations, in various chemical processes and in the newly developed mercury turbine, it has become important to have a method whereby leaks in apparatus and traces of mercury vapor in the atmosphere can be detected quickly. Previous methods of determining the amount of mercury vapor in the atmosphere were tedious processes that required considerable time and the services of an expert chemist, and even then the results were usually far from accurate, especially when considering minute amounts of the substance. The new method gives quick results, does not require chemical training to carry out, and is accurate.

The principle on which the new method is based is a reaction between a solid substance, selenium sulphide, and the mercury vapor, with the reaction product a colored substance easily observable with the eye. The yellow selenium sulphide is applied as a coating on paper. The paper is blackened on exposure to air containing mercury vapor, the degree of blackening depending on the concentration of the mercury, the time of exposure, and various other factors which can be definitely controlled. For continuous and automatic registration of the mercury vapor, there has been devised a system in which a continuous strip of the coated paper is drawn slowly over an opening through which the air flows, a small clock motor moving the strip of paper at a uniform rate. A short time after the exposure, the colored strip of paper can be compared with a standard scale, in which the different shades from yellow to black have been calibrated in terms of mercury concentration.

If an incandescent lamp is placed in front of the strip of paper and a photoelectric cell behind it, the amount of light reaching the cell will depend on the amount of blackening of the paper. The light can regulate the readings of an ammeter, so that the concentration of the mercury vapor can be determined either by observing the color of the paper or by reading the ammeter. It is also possible to so arrange the photoelectric cell circuit that, should the mercury concentration become dangerously high, a warning gong will be sounded.

GENERAL ELECTRIC COMPANY